

# COUNTS: Benchmarking Object Detectors and Multimodal Large Language Models under Distribution Shifts

Jiansheng Li<sup>†</sup>, Xingxuan Zhang<sup>†</sup>, Hao Zou, Yige Guo, Renzhe Xu, Yilong Liu  
 Chuzhao Zhu, Yue He, Peng Cui\*

Department of Computer Science, Tsinghua University

lijjs23@mails.tsinghua.edu.cn, cuiip@tsinghua.edu.cn

## Abstract

*Current object detectors often suffer significant performance degradation in real-world applications when encountering distributional shifts. Consequently, the out-of-distribution (OOD) generalization capability of object detectors has garnered increasing attention from researchers. Despite this growing interest, there remains a lack of a large-scale, comprehensive dataset and evaluation benchmark with fine-grained annotations tailored to assess the OOD generalization on more intricate tasks like object detection and grounding. To address this gap, we introduce COUNTS, a large-scale OOD dataset with object-level annotations. COUNTS encompasses 14 natural distributional shifts, over 222K samples, and more than 1,196K labeled bounding boxes. Leveraging COUNTS, we introduce two novel benchmarks: O(OD)<sup>2</sup> and OODG. O(OD)<sup>2</sup> is designed to comprehensively evaluate the OOD generalization capabilities of object detectors by utilizing controlled distribution shifts between training and testing data. OODG, on the other hand, aims to assess the OOD generalization of grounding abilities in multimodal large language models (MLLMs). Our findings reveal that, while large models and extensive pre-training data substantially enhance performance in in-distribution (IID) scenarios, significant limitations and opportunities for improvement persist in OOD contexts for both object detectors and MLLMs. In visual grounding tasks, even the advanced GPT-4o and Gemini-1.5 only achieve 56.7% and 28.0% accuracy, respectively. We hope COUNTS facilitates advancements in the development and assessment of robust object detectors and MLLMs capable of maintaining high performance under distributional shifts.*

## 1. Introduction

Extensive literature demonstrates that when the independent and identically distributed (IID) assumption between training and test data is violated, existing models may experience significant performance degradation [27, 36, 80, 101]. Even current multimodal large language models (MLLMs)[1, 3, 15, 61, 74] exhibit limited out-of-distribution generalization capabilities, severely hindering their usability and trustworthiness in specific domains [22, 87, 97].

The challenges inherent in out-of-distribution (OOD) generalization have spurred significant research interest. However, existing efforts have predominantly centered on image classification tasks [21, 36, 43], leaving a considerable gap in our understanding of how models perform on more intricate, real-world tasks. Furthermore, while recent works on MLLMs have aimed for comprehensive evaluation [4, 53, 92], they often neglect the crucial aspect of grounding model responses within the visual context. This grounding is indispensable for sophisticated applications such as detailed visual comprehension, interactive embodied agents, and localized content manipulation. Recent advancements allowing models to process user-specified regions via bounding boxes represent a promising direction [66], but a thorough investigation of grounding abilities from an OOD generalization perspective remains an open research area. This underscores the need for novel benchmarks and datasets specifically designed to rigorously assess these critical facets of model performance.

This discrepancy can be attributed to the scarcity of suitable benchmark datasets. While comprehensive benchmarks for classification tasks abound [26, 28, 36, 63], there is a dearth of robust benchmarks offering finer-grained annotations. Previous studies have often relied on synthetically corrupted data for robustness evaluation [59], but the extent to which such simulations accurately reflect real-world scenarios remains debatable. Consequently, other research has turned to collecting images from the

---

<sup>†</sup>Equal Contribution, \*Corresponding Author

<sup>2</sup>Code and Dataset are available at [https://github.com/jiansheng-li/COUNTS\\_benchmark](https://github.com/jiansheng-li/COUNTS_benchmark).

internet to construct datasets. For example, road scene datasets [11, 16, 33, 88] have been employed to benchmark the domain generalization of detectors [25, 35, 45, 104]. However, such scene-specific datasets lack generalizability and domain diversity, potentially leading to biased robustness assessments. Moreover, recent efforts have sought to analyze the out-of-distribution generalization capabilities of MLLMs [22, 97]. Nonetheless, due to the absence of appropriate benchmarks, these studies have primarily focused on simple image-level classification tasks [32], neglecting the investigation of fine-grained visual grounding generalization in large models.

In this work, we introduce Common Objects UNder disTribution Shifts (COUNTS), a large-scale finely annotated dataset designed for OOD generalization research. COUNTS comprises 14 distinct domains, 35 categories, and 222,234 samples, all derived from real-world images and meticulously labeled through a combination of automated pipelines and human annotation. As the first real-world dataset to support both training and testing of OOD generalization for object detection and grounding tasks, COUNTS enables us to propose two novel benchmarks: OOD in Object Detection ( $O(OD)^2$ ) for evaluating object detectors and OOD Grounding (OODG) for assessing the grounding generalization capabilities of MLLMs.

In OODG, given the lack of transparency regarding MLLMs’ training data, we define distribution shift as the discrepancy between few-shot examples (in-context learning) and test samples. This definition reflects the real-world usage of MLLMs, where users typically provide prompts and examples before deployment, underscoring the importance of generalization based on given information.

We propose five settings in OODG:

**1. Zero-shot capability** assesses the MLLM’s zero-shot grounding ability across diverse domains.

**2. ICL with IID samples** evaluates the MLLM’s performance when the in-context examples (ICE) and test samples are independent and identically distributed.

**3. Generalization under covariate shifts** examines the MLLM’s generalization ability when faced with unknown input sample distributions.

**4. Generalization under label shifts** investigates the MLLM’s generalization ability when faced with unknown test label distributions.

**5. Generalization under spurious correlation shifts** assesses the MLLM’s generalization ability on unknown test sample distributions when spurious correlations between visual features and labels exist in the ICE.

Our contributions are summarized as follows:

- We introduce COUNTS, the first large-scale dataset with fine-grained annotations specifically designed to support both object detection and grounding tasks under natural distribution shifts.

- We propose  $O(OD)^2$ , a benchmark for evaluating the OOD generalization capabilities of object detectors using COUNTS. Through comprehensive analysis, we identify common factors that contribute to model robustness, providing insights that can inform the development of more resilient detection algorithms.
- We introduce OODG, a benchmark with five distinct settings designed to assess the OOD generalization of grounding abilities in MLLMs. Leveraging COUNTS, we investigate the impact of ICL distribution shifts on the grounding performance of MLLMs.

## 2. Related Works

In this section, we briefly review the previous works on object detection and multimodal large language models.

**Object Detection** There have been large amounts of literature proposing the models and benchmarks of object detectors. The models of object detectors can be categorized into two classes, that are single-stage detectors [48, 50, 73, 75, 102] and two-stage detectors [18, 19, 24, 47, 69]. They usually relies on the convolutional layer [39] to extract the representation of images. Recently, motivated by the advancement of transformer architecture [76], many transformer-based object detectors [7, 105] are proposed. To evaluate the performance of the various object detector, several datasets are proposed, such as COCO [46] and VOC [13]. However, in the wild scenarios, the object detectors may face the impact of corruption and distribution shifts. To incorporate these factors into consideration, COCO-C [59] and COCO-O [55] are sequentially proposed. COCO-C adds synthetic corruptions into the images of COCO to obtain the perturbated images. COCO-O aims to evaluate the out-of-distribution generalization of detectors and account for natural distribution shift.

**Multimodal Large Language Models** In recent years, many multimodal large language models are developed to jointly encode vision and language [10, 44, 65, 72, 94]. They are pre-trained with massive amount of vision data and text on the web. As these multimodal large language models evolve, they are becoming increasingly excelling in understanding the content combining visual and textual information. Based on the pre-trained large models, instruction-tuning [2, 29, 41, 60, 99] can be applied and improve their capability of instruction following. Researchers can harness the power of multimodal large language models to conduct grounding [66] and provide insightful answers to questions pertaining to images, such as the object information in the images.

**Benchmark of MLLM** To assess the capabilities of multimodal large language models, the research community has developed massive amount of benchmarks. Some benchmarks focus on the single-task evaluation. For example, VQA [20], OK-VQA [56], and GQA [30] are all

dedicated to the pursuit of excellence in the domain of visual question answering. To compensate the insufficiency of these benchmarks in holistical assessment of multimodal large language models [40, 51, 51, 86, 91, 91], numerous benchmarks are proposed to evaluate the other aspect of the models, including adversarial robustness [100], hallucination [12], mathematical ability [53] and multimodality handling [57, 92]. Although these benchmarks inspect the capabilities of multimodal large language models in different tasks, they neglect the impact of distribution shift, which is the focus of this paper.

### 3. The COUNTS Dataset

#### 3.1. Overview of COUNTS

We introduce Common Objects UNder disTribution Shifts (COUNTS), a large-scale, fine-grained annotated dataset designed to facilitate the training and evaluation of traditional object detectors, as well as to assess the OOD grounding capabilities of MLLMs. COUNTS encompasses 35 object categories (visual concepts), 14 distinct domains, 222,234 images, and 1,196,114 annotated bounding boxes. All images in COUNTS are sourced from real-world scenes, ensuring the absence of artificially generated samples. As noted in prior work [55, 96], naturally occurring distribution shifts more accurately reflect the challenges encountered in real-world applications, while also presenting greater potential for meaningful solutions. Furthermore, each domain within COUNTS includes the full spectrum of object categories, guaranteeing the validity of cross-distribution testing.

COUNTS provides significant distribution shifts to support the evaluation of OOD generalization abilities. Example images are shown in Figure 1. Existing OOD generalization datasets primarily focus on classification tasks, limiting their ability to examine fine-grained spatial visual information. Different domains may differentially impact various regions within the same image (e.g., areas with varying snow thickness), posing greater challenges for models to perceive visual information at a spatially granular level. Additionally, COUNTS’s ability to support the training of detectors, coupled with its abundance of domains and categories, allows for the creation of controlled distribution shifts by adjusting the training and testing distributions.

#### 3.2. domain Selection

To ensure that the selected domains accurately reflect the data distributions likely encountered in real-world model deployment, we focused on domains that are prevalent in real-world scenarios and have the potential to significantly impact image pixel distributions, while also striving for mutual independence among the chosen domains. Ultimately, we identified 14 domains: *dim, painting, snow, sand, hand-*

*made, street, road, water, grass, indoor, mountain, sky, tree,* and *occlusion*. These domains are frequently encountered in daily life and are likely to exhibit distinct associations with objects. It is important to note that objects within the samples are typically in the foreground, while domains often serve as background elements or overall image attributes. Therefore, we annotate domains at the image level, while bounding boxes are provided at the object level. A more comprehensive description and additional information regarding these domains can be found in Appendix A.

#### 3.3. Data Collection

We primarily employed a three-stage data selection and annotation process. In the first stage, we conduct an initial screening of publicly available image datasets containing image captions, based on our predefined domain space. We consider Open Images [38], Visual Genome (VG) [37], RefCOCO [34], RefCOCO+ [34], RefCOCOg [90], Flickr30K [64], and GranD [66]. In total, more than 5 million images with domains are initially screened. In the second stage, we engaged human annotators to verify and annotate the domain information of the selected images. Only samples that were consistently identified as belonging to the same domain by two independent annotators were retained and the labeled domain is considered as the ground-truth domain for each image. In the third stage, we randomly sampled 10% of the data within each domain to form the test and validation sets. We observe that datasets such as Open Images and GranD contained automatically annotated data, resulting in incomplete or inaccurate bounding box annotations for some objects. Our experiments reveal that training detectors on data with incomplete bounding box annotations did not significantly impact their performance. Conversely, incomplete or inaccurate annotations in the test or validation sets notably affected the reliability of the test results. Therefore, we employ human annotators to meticulously re-annotate the bounding boxes in the test and validation sets, ensuring that each object is labeled and verified by two independent annotators. A total of 23,000 images are re-annotated with bounding boxes by annotators. Please see more details in Appendix A.

#### 3.4. Comparison with Existing Benchmarks

To further distinguish COUNTS from existing OOD generalization benchmarks, Table 1 provides a comparative overview of relevant dataset characteristics. While current large-scale OOD benchmarks predominantly focus on image classification, those offering finer-grained annotations (e.g., object detection) tend to be limited in scope. Existing datasets often lack either a sufficient diversity of domains to thoroughly assess OOD generalization capabilities or the scale necessary to support robust detector training and controlled experimentation with distribution shifts. COUNTS

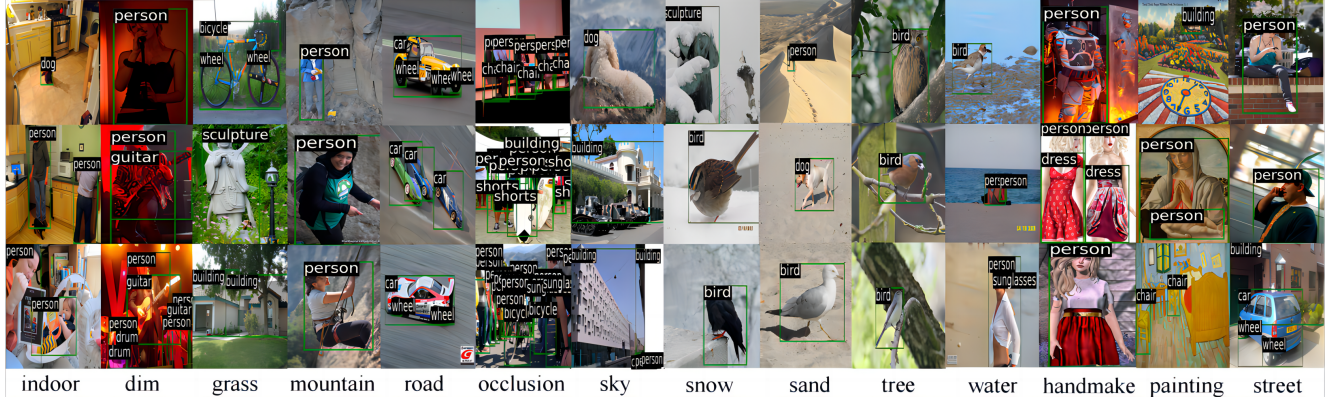


Figure 1. Examples of images in COUNTS. Each image is annotated with domain and objects.

addresses these limitations by offering a substantial number of diverse domains, a vast corpus of natural images, and high-quality fine-grained annotations. This unique combination enables researchers to explore a wider range of advanced and complex OOD generalization tasks within the visual domain, including those requiring precise object localization and detection under varying conditions.

## 4. Benchmarks

### 4.1. OOD in Object Detection (O(OD)<sup>2</sup>)

O(OD)<sup>2</sup> is designed to assess the OOD generalization capabilities of existing object detectors and to investigate the key factors that influence their generalization performance, thereby providing insights for future advancements.

Given the strong performance of current detectors under IID conditions, we specifically focus on their performance in unknown domains where the test domains do not overlap with the training domains. As COUNTS maintains a consistent category space across all domains, we utilize the full set of categories for both training and testing phases.

Furthermore, prior research suggests that evaluating models on multiple target distributions, rather than a single one, more accurately reflects real-world scenarios with numerous potential unknown distributions and mitigates the risk of unfairness caused by target distribution information leakage [89, 96]. Consequently, we employ multiple domains as target domains, with the remaining domains serving as the training set. Specifically, in the main paper, we adopt *sky*, *occlusion*, *grass*, *water*, *dim*, and *handmake* as the target domains due to their representation of diverse distribution shift patterns. For example, the *sky* domain presents challenges due to the high variability in angle and lighting conditions. The *occlusion* domain tests the model’s robustness to partial or complete object obstruction, while the *grass* and *water* domains introduce complex backgrounds with varying textures and reflections. The *dim* domain

evaluates performance under low-light conditions, and the *handmake* domain assesses generalization to artistic renditions or sketches of objects.

### 4.2. OOD in Grounding (OODG)

With OODG, we investigate the generalization abilities of MLLMs in the context of grounding tasks, a critical component for various real-world applications such as autonomous driving and visual perception in autonomous systems.

Currently, there is no universally accepted definition for OOD generalization in MLLMs. Traditional OOD generalization approaches rely on artificially constructed distribution shifts between training and test data. However, due to the unknown nature of current MLLMs’ pre-training and fine-tuning data, it is challenging to characterize the distribution shifts between their training and test data.

Given the limited information available regarding the pre-training and fine-tuning data of many MLLMs, we propose to define distribution shifts within the ICL stage. This approach allows us to examine the generalization capabilities of MLLMs when there are distribution shifts between the ICE and the actual test samples. This setting is well-justified, as MLLM parameters remain fixed in many applications, and defining distribution shifts during ICL enables assessment of their generalization to diverse scenarios in real-world deployment. It is worth noting that COUNTS contains a sufficient amount of high-quality data to support fine-tuning the grounding capabilities of MLLMs. This opens up the possibility of investigating the models’ generalization abilities when distribution shifts occur between the fine-tuning data and test data. However, this is not the primary focus of this work.

We utilize data from the human-annotated test and validation sets to construct the evaluation framework for this problem. We primarily consider three testing scenarios:

**1. Visual Grounding.** Given an image and a region of interest, we query the multimodal large language model and

Datasets	Task	Domain Num.	Class Num.	Natural Images	Images / Domain
PACS[42]	Classification	4	7	9,991	2,497
VLCS[14]		4	5	10,729	2,682
Officehome[77]		4	65	15,588	3,897
DomainNet[63]		<b>6</b>	<b>345</b>	<b>586,575</b>	<b>97,762</b>
OOD-CV[98]	Object Detection& Grounding	5	10	2,632	526
Comic2k[31]		1	6	2,000	2,000
Clipart[31]		1	20	1,000	1,000
Watercolor[31]		1	6	2,000	2,000
COCO-C[58]		<b>15</b>	<b>80</b>	0	0
COCO-O[54]		6	<b>80</b>	6,782	1,130
COUNTS (ours)		14	35	<b>222,234</b>	<b>15,874</b>

Table 1. Overview of current OOD generalization and robust detection benchmarks.

assess the accuracy of its textual response.

**2. Recognition and Localization.** Given an image and a question, we evaluate the accuracy of the model’s predicted bounding box coordinates for the relevant region.

**3. Visual and Semantic Mapping.** Given an image and a sequence of textual descriptions, we assess the accuracy of the model’s ability to map the descriptions to the corresponding regions in the image.

For generalization evaluation, we consider five distinct settings:

**1. Zero-shot Generalization.** This setting investigates the ability of MLLMs to recognize visual concepts across various domains without any prior examples. **2. I.I.D. ICL.** This setting examines the i.i.d. generalization capability of MLLMs when provided with examples drawn from the same distribution as the test data.

**3. ICL with Covariate Shifts.** This setting explores the impact of covariate shifts between in-context examples and test samples on model performance. It aligns with existing OOD generalization research, where examples and test samples originate from different domains, to assess the model’s ability to generalize to unseen sample distributions. **4. ICL with Label Shifts.** This setting investigates the generalization capability of MLLMs when label shifts exist between in-context examples and test samples. It aims to determine whether the distribution of labels in the examples significantly affects model performance when the distribution of visual concepts in the test data is unknown.

**5. ICL with Spurious Correlation Shifts.** This setting examines whether MLLMs are misled by spurious correlations between image features and descriptions in the in-context examples, causing them to overlook more fundamental relationships. Specifically, due to sampling bias, providing ICL samples may introduce statistical associations between irrelevant features and descriptions. For instance, if the concept *cat* frequently appears in darker indoor settings while *dog* appears predominantly outdoors in the ICL samples, a spurious correlation may arise between dim lighting and the concept *cat* or between

outdoor environments and the concept *dog*. This could lead to erroneous predictions when the model encounters a cat in an outdoor setting.

## 5. Experiments

### 5.1. OOD in Object Detection

For O(OD)<sup>2</sup>, we employ representative object detectors spanning two distinct architectures: the two-stage Faster R-CNN [69] and the one-stage detectors RetinaNet [48] and YOLOv9 [78]. All experiments were conducted using the MMDetection framework, adhering to the optimal training configurations specified in the respective original publications. The computational resources for this benchmark consisted of NVIDIA RTX 4090 GPUs. We investigate the impact of various advanced model architectures on the OOD generalization capabilities of object detectors, focusing on the backbone, neck, and head components. All experiments investigating model structures begin by training detectors from initial parameters pre-trained on ImageNet, ensuring a fair comparison across architectures. To further explore the influence of pre-training data on a detector’s OOD generalization ability, we utilize diverse pre-training datasets for model initialization on representative model structures. Introduction of the evaluated models and more experimental setups such as training hyperparameter selection are detailed in Appendix B.

The main results of O(OD)<sup>2</sup> with various detector architectures and models are shown in Table 2. Existing detectors exhibit limited OOD generalization capabilities and improvements in IID performance do not necessarily translate to enhanced OOD generalization. Performance across various OOD scenarios was notably suboptimal compared with their performance on IID benchmarks. In some cases, IID improvements may even negatively impact OOD performance. For example, with stronger neck NAS-FPN and head FreeAnchor, the detectors show weaker generalization across domains.

For two-stage detectors, modifications to the head archi-

		VAL mAP	Test mAP							Avg		
			Sky	Occlusion	Grass	Water	Dim	Handmake				
Two-stage Detector	Faster R-CNN	RN-50 [23]	0.279	0.178	0.139	0.156	0.103	0.140	0.134	0.135		
		RN-101 [23]	<b>0.325</b>	<b>0.212</b>	0.143	0.166	<b>0.110</b>	0.152	<b>0.144</b>	0.148		
		Backbone RX-101-32x4d [85]	0.310	0.200	<b>0.163</b>	<b>0.179</b>	0.109	<b>0.159</b>	0.132	<b>0.150</b>		
		Swin-T [52]	0.308	0.192	0.158	0.163	0.102	0.155	0.129	0.142		
		PVTv2-B2 [82]	0.303	0.189	0.156	0.161	0.103	0.153	0.126	0.141		
	Neck	FPN [47]	0.279	0.178	0.139	0.156	0.103	<b>0.140</b>	<b>0.134</b>	0.135		
		PAFPN [49]	<b>0.309</b>	0.184	<b>0.148</b>	<b>0.158</b>	0.140	0.109	0.119	<b>0.140</b>		
		NAS-FPN [17]	0.298	<b>0.186</b>	0.141	0.153	<b>0.143</b>	0.108	0.113	0.136		
	Head	Standard	0.279	0.178	0.139	0.156	0.103	0.140	0.134	0.135		
		Cascade [5]	0.339	0.193	0.162	0.172	0.111	0.154	0.146	0.149		
		SABL [79]	<b>0.347</b>	<b>0.218</b>	<b>0.177</b>	<b>0.182</b>	0.135	<b>0.165</b>	<b>0.158</b>	<b>0.162</b>		
		2_Heads [84]	0.308	0.197	0.163	0.163	0.120	0.150	0.133	0.149		
		Groie [71]	0.309	0.188	0.153	0.164	<b>0.148</b>	0.150	0.131	0.141		
One-stage Detector	RetinaNet	RN-50 [23]	0.331	0.199	0.189	0.166	0.108	0.179	<b>0.149</b>	0.156		
		RN-101 [23]	0.342	<b>0.203</b>	<b>0.194</b>	0.175	0.110	<b>0.192</b>	<b>0.149</b>	<b>0.162</b>		
		Backbone RX-101-32x4d [85]	0.302	0.189	0.158	0.169	0.104	0.147	0.131	0.144		
		Swin-T [52]	<b>0.340</b>	0.201	0.191	<b>0.179</b>	<b>0.117</b>	0.188	0.146	<b>0.162</b>		
		PVTv2-B2 [82]	0.338	0.192	0.184	0.175	0.109	0.183	0.143	0.158		
	Neck	FPN [47]	0.331	0.199	<b>0.189</b>	<b>0.166</b>	0.108	<b>0.179</b>	<b>0.149</b>	0.156		
		PAFPN [49]	<b>0.339</b>	<b>0.205</b>	0.178	<b>0.166</b>	<b>0.123</b>	0.162	0.138	<b>0.157</b>		
		NAS-FPN [17]	0.306	0.146	0.141	0.157	0.113	0.128	0.127	0.133		
	Head	Standard	0.331	0.199	<b>0.189</b>	0.166	0.108	<b>0.179</b>	0.149	0.156		
		SABL [79]	<b>0.345</b>	<b>0.214</b>	<b>0.189</b>	<b>0.180</b>	<b>0.141</b>	0.168	<b>0.156</b>	<b>0.161</b>		
		FSAF [103]	0.332	0.174	0.172	0.168	0.123	0.162	0.127	0.153		
	FreeAnchor [95]		0.298	0.166	0.115	0.163	0.111	0.138	0.116	0.131		
<b>YOLO V9</b> [78]			0.282	0.190	0.118	0.160	0.120	0.153	0.121	0.150		
<b>DETR</b> [6]			0.348	0.211	0.183	0.185	0.121	0.209	0.159	0.168		
<b>DINO</b> [8]			0.384	<b>0.250</b>	<b>0.250</b>	0.229	<b>0.169</b>	0.212	<b>0.181</b>	<b>0.213</b>		
<b>DINO V2</b> [62]			<b>0.389</b>	0.252	0.249	<b>0.231</b>	0.165	<b>0.213</b>	<b>0.181</b>	<b>0.213</b>		

Table 2. Comparison of object detectors with different backbone, neck, and head. The best results of components for each detector are highlighted in bold font.

ture yield more significant improvements than strengthening the backbone. For one-stage detectors, both stronger backbones and heads contribute to improved results. This suggests that the head can be the key to learning strong local representations and reducing environmental impacts. Thus optimizing the head design may be a more effective strategy for enhancing OOD generalization. Moreover, improvements in the neck architecture have limited impacts on OOD generalization. Among all evaluated models, DINO and DINOv2 demonstrated the most favorable performance, significantly outperforming other detectors. This suggests that, in addition to model architecture, training strategies can exert a substantial influence on a model’s OOD generalization capabilities.

In Table 3, we analyze the impact of pre-training data and methods on the OOD generalization capabilities of object detectors. Our findings reveal that increasing the size of pre-training data or employing self-supervised pre-training methods does not yield significant improvements in generalization. However, utilizing advanced training method-

ologies can substantially enhance model performance. For instance, Sup\_timm [83], when trained on the same data, achieves a 2.67% absolute improvement in mean average precision (mAP) and an 18.9% relative improvement compared to traditional ImageNet pre-training.

## 5.2. OOD in Grounding

For OODG, we evaluated state-of-the-art multimodal large models including GPT-4, Gemini 1.5, and Claude 3. Due to space constraints, we focus on Visual Grounding and Recognition and Localization and primarily present results for GPT-4 and Gemini 1.5 Flash in the main body of this paper, with additional findings provided in Appendix C.

- **Visual Grounding.** In order to study the ability of multimodal large models to perform grounding within given regions, we implemented a methodology involving the use of highlighted bounding boxes to delineate objects or backgrounds within images. We then assessed the accuracy of the models’ returned visual concepts. To ensure a thorough evaluation of visual

	Backbone method	Pretraining Data	VAL mAP	mAP on COUNTS								Avg
				Sky	Occlusion	Grass	Water	Dim	Handmake			
Two-stage	Faster R-CNN	Supervised	IN-1k	0.301	0.193	0.140	0.153	0.112	0.148	0.136	0.141	0.141
		Sup_timm [83]	IN-1k	<b>0.323</b>	<b>0.210</b>	<b>0.147</b>	<b>0.161</b>	<b>0.118</b>	<b>0.165</b>	<b>0.139</b>	<b>0.167</b>	0.145
		MoCov2 [9]	IN-1k	0.298	0.193	0.136	0.148	0.114	0.139	0.118	0.136	0.136
		Supervised	IN-21k [70]	0.313	0.201	0.142	0.158	0.114	0.152	0.134	0.146	0.146
One-stage	RetinaNet	Supervised	IN-1k	0.309	0.197	0.143	0.156	0.113	0.151	0.139	0.145	0.145
		Sup_timm [83]	IN-1k	<b>0.325</b>	<b>0.214</b>	<b>0.149</b>	<b>0.162</b>	<b>0.123</b>	<b>0.170</b>	<b>0.142</b>	<b>0.170</b>	0.145
		MoCov2 [9]	IN-1k	0.303	0.189	0.131	0.144	0.112	0.135	0.116	0.133	0.133
		Supervised	IN-21k [70]	0.313	0.201	0.142	0.158	0.114	0.152	0.134	0.146	0.146

Table 3. Comparison of object detectors with different backbone and pretraining methods.

Setting	Model	ICE	Sky			Occlusion			Water			Dim			Handmake			Overall
			S	M	L	S	M	L	S	M	L	S	M	L	S	M	L	
1	GPT-4o	0	0.434	<b>0.727</b>	0.889	0.362	<b>0.891</b>	<b>0.805</b>	<b>0.554</b>	0.797	0.860	<b>0.626</b>	0.727	0.737	<b>0.353</b>	0.595	0.535	<b>0.659</b>
	Gemini-1.5-Flash	0	<b>0.444</b>	0.667	0.778	0.355	0.674	0.628	0.533	0.783	0.858	0.347	0.716	0.570	0.333	<b>0.608</b>	<b>0.575</b>	0.591
	GLaMM [67]	0	0.333	0.667	<b>1.000</b>	<b>0.387</b>	0.714	0.444	<b>0.554</b>	<b>0.857</b>	<b>1.000</b>	0.429	<b>0.857</b>	<b>0.857</b>	0.333	0.429	0.513	0.625
	Qwen2-VL [81]	0	0.286	0.667	0.889	0.333	0.667	0.355	0.533	0.667	0.750	0.385	0.625	0.714	0.286	0.444	0.555	0.544
2	GPT-4o	1	<b>0.445</b>	0.778	0.778	<b>0.571</b>	<b>1.000</b>	<b>1.000</b>	0.143	0.429	<b>1.000</b>	<b>0.333</b>	0.771	0.750	0.000	0.680	<b>1.000</b>	0.646
		2	<b>0.445</b>	0.667	0.778	0.143	<b>0.857</b>	<b>1.000</b>	<b>0.554</b>	0.797	0.860	<b>0.333</b>	0.778	0.778	0.000	<b>0.825</b>	<b>1.000</b>	0.654
	Gemini-1.5-Flash	1	0.444	0.714	<b>1.000</b>	0.143	<b>1.000</b>	0.857	0.286	<b>0.857</b>	<b>1.000</b>	0.222	<b>1.000</b>	<b>0.889</b>	0.000	0.637	<b>1.000</b>	0.670
		2	0.444	<b>0.857</b>	<b>1.000</b>	0.143	<b>1.000</b>	0.143	<b>0.857</b>	<b>1.000</b>	<b>0.333</b>	<b>1.000</b>	<b>0.889</b>	0.000	0.671	<b>1.000</b>	<b>0.689</b>	
3	GPT-4o	1	0.143	0.357	<b>0.857</b>	0.357	0.786	<b>0.929</b>	0.143	0.429	0.786	0.222	0.722	0.667	0.000	<b>0.889</b>	<b>1.000</b>	0.552
		2	<b>0.429</b>	<b>0.556</b>	0.492	<b>0.385</b>	<b>1.000</b>	<b>0.929</b>	0.143	0.429	<b>0.929</b>	<b>0.278</b>	<b>0.778</b>	<b>0.778</b>	0.000	0.714	<b>1.000</b>	<b>0.589</b>
	Gemini-1.5-Flash	1	0.222	0.143	0.143	0.143	0.143	0.143	<b>0.286</b>	<b>0.714</b>	0.857	0.111	0.444	0.444	0.000	0.571	<b>1.000</b>	0.358
		2	0.000	0.000	0.222	0.143	0.143	0.143	<b>0.286</b>	<b>0.714</b>	0.857	0.222	0.444	0.444	0.000	0.571	<b>1.000</b>	0.346
4	GPT-4o	1	0.133	<b>0.286</b>	<b>1.000</b>	0.429	<b>0.857</b>	<b>0.857</b>	<b>0.286</b>	0.429	<b>0.857</b>	0.000	0.556	0.667	<b>0.342</b>	0.432	<b>1.000</b>	<b>0.533</b>
		2	<b>0.143</b>	<b>0.286</b>	<b>1.000</b>	0.286	0.571	<b>0.857</b>	<b>0.286</b>	0.429	<b>0.857</b>	<b>0.111</b>	<b>0.667</b>	<b>0.778</b>	0.000	0.424	<b>1.000</b>	0.503
	Gemini-1.5-Flash	1	0.000	0.111	0.143	0.111	0.133	0.127	<b>0.286</b>	0.857	<b>0.857</b>	<b>0.111</b>	0.222	0.222	0.000	<b>0.714</b>	<b>1.000</b>	0.317
		2	0.111	0.111	0.143	0.111	0.137	0.111	<b>0.286</b>	<b>1.000</b>	0.714	0.000	0.222	0.222	0.000	0.424	<b>1.000</b>	0.297
5	GPT-4o	4	0.286	0.500	<b>0.917</b>	0.308	0.444	<b>0.833</b>	<b>0.375</b>	0.556	<b>0.750</b>	0.333	0.588	0.769	0.133	0.352	0.462	0.507
		8	<b>0.714</b>	0.875	0.833	0.311	<b>0.556</b>	<b>0.833</b>	0.313	<b>0.778</b>	<b>0.750</b>	0.143	<b>0.800</b>	<b>0.923</b>	0.266	<b>0.412</b>	0.625	<b>0.609</b>
	Gemini-1.5-Flash	4	0.500	0.875	0.888	0.534	0.473	0.500	<b>0.375</b>	0.556	<b>0.750</b>	<b>0.347</b>	0.716	0.570	0.400	0.313	<b>0.769</b>	0.571
		8	0.467	<b>0.889</b>	0.875	<b>0.690</b>	0.544	0.812	0.313	<b>0.778</b>	<b>0.750</b>	<b>0.347</b>	0.716	0.570	<b>0.467</b>	0.353	0.462	0.602

Table 4. Results of Visual Grounding. The selection accuracy of MLLMs is reported. S, M, and L indicate small, medium, and large objects, respectively.

recognition across a wide range of region types, we included all categories and domains as potential visual concepts, reporting accuracy rates for small ( $<32 \times 32$ ), medium (from  $32 \times 32$  to  $96 \times 96$ ), and large ( $>96 \times 96$ ) bounding boxes. A multiple-choice approach was employed, wherein all possible answers were presented in the prompt, and the accuracy of the model’s selected visual concept was verified. Further details regarding prompt design and experimental specifics can be found in Appendix B.

- Recognition and Localization. To assess the capability of MLLMs to perceive and comprehend comprehensive visual information within images, we designed a task wherein the MLLM is prompted to return the bounding box coordinates of specified visual elements. Input images were uniformly resized to a standardized resolution ( $448 \times 448$ ) to mitigate potential errors arising from

variations in image resolution and dimensions. We report the model’s performance across all categories and domains, as well as its mean average precision (mAP) on small, medium, and large bounding boxes.

**Zero-shot Generalization.** We show the main results of Visual Grounding and Recognition and Localization in Table 4 and 5, respectively. While current MLLMs demonstrate strong performance on image-level tasks, their performance on fine-grained grounding tasks remains suboptimal. Notably, both GPT-4o and Gemini-1.5 exhibit limitations when dealing with objects characterized by very small or very large bounding boxes, indicating a need for further enhancement of their localized perception capabilities. For instance, in the visual grounding task, GPT and Gemini achieve recognition accuracies of 35.3% and 33.3%, respectively, on small-sized bounding boxes within the *handmake*

Setting	Model	ICE	Occlusion			Dim			Handmake			Overall
			S	M	L	S	M	L	S	M	L	
1	GPT-4o	0	<b>0.108</b>	<b>0.099</b>	<b>0.112</b>	<b>0.108</b>	<b>0.099</b>	<b>0.112</b>	<b>0.108</b>	<b>0.099</b>	<b>0.112</b>	<b>0.106</b>
	Gemini-1.5-Flash	0	0.083	0.091	0.090	0.101	<b>0.099</b>	0.083	0.100	0.002	0.089	0.082
2	GPT-4o	1	<b>0.113</b>	<b>0.068</b>	<b>0.101</b>	0.079	0.101	0.086	<b>0.099</b>	0.071	0.100	<b>0.091</b>
	Gemini-1.5-Flash	2	0.108	0.059	0.099	<b>0.083</b>	0.098	0.083	<b>0.099</b>	0.068	<b>0.101</b>	0.089
3	GPT-4o	1	<b>0.041</b>	<b>0.035</b>	0.016	<b>0.008</b>	0.001	<b>0.072</b>	0.000	<b>0.019</b>	<b>0.053</b>	<b>0.027</b>
	Gemini-1.5-Flash	2	0.040	0.015	<b>0.032</b>	0.006	<b>0.004</b>	0.065	0.000	0.011	0.038	0.023
4	GPT-4o	1	<b>0.036</b>	0.020	<b>0.101</b>	0.009	0.014	0.003	0.100	0.018	<b>0.101</b>	<b>0.045</b>
	Gemini-1.5-Flash	2	0.029	0.018	0.029	<b>0.019</b>	0.010	0.013	0.049	<b>0.058</b>	0.017	0.027
5	GPT-4o	4	<b>0.019</b>	0.028	0.013	<b>0.025</b>	<b>0.010</b>	0.009	0.053	<b>0.091</b>	0.008	0.028
	Gemini-1.5-Flash	8	0.002	<b>0.104</b>	<b>0.016</b>	0.018	<b>0.010</b>	<b>0.029</b>	<b>0.084</b>	0.016	<b>0.009</b>	<b>0.032</b>
		4	0.000	0.000	0.000	0.000	0.000	0.000	0.000	0.000	0.000	0.000
		8	0.000	0.000	0.000	0.000	0.000	0.000	0.000	0.000	0.000	0.000

Table 5. Results of Recognition and Localization. mAP is reported.

domain, markedly lower than other results. In the Recognition and Localization task, both GPT-4o and Gemini-1.5-Flash show weak generalization and are still quite far from being usable.

**ICL with IID Samples.** Our findings reveal that incorporating ICE drawn from the same distribution as the test samples significantly enhances Gemini’s performance on visual grounding tasks. This improvement becomes more pronounced with increasing ICE quantity (see Appendix C for results with varying ICE counts). Conversely, GPT does not exhibit a similar enhancement.

**ICL under Covariate / Concept / Spurious Correlation Shifts.** Introducing distribution shifts, such as covariate and label shifts, into the ICE leads to a notable degradation in Gemini’s performance compared to zero-shot learning. In the Visual Grounding task, average accuracy drops from a maximum of 57.0% to 28.0%, representing a relative decrease of 50.88%. While GPT-4o also experiences a performance decline, it is less severe, with a maximum decrease of 12.1%.

These results highlight two critical conclusions:

**1. Defining distribution shifts within the ICL phase is both valid and impactful.** This aligns with typical MLLM usage scenarios and is supported by our empirical findings, which demonstrate the substantial influence of ICL distribution shifts on model performance. Notably, covariate shift, a non-adversarial and naturally occurring distribution shift, closely approximates real-world applications [96]. The presence of such shifts within ICL can lead to model per-

formance significantly below zero-shot levels, underscoring the importance of careful ICE data preparation and further research to mitigate the negative impact of ICL distribution shifts on generalization.

**2. How MLLMs leverage ICL to learn reliable knowledge is a crucial question.** Consistent with our findings in IID experiments, Gemini appears to extract more information from ICE compared to GPT-4o. While beneficial under IID ICL conditions, this becomes detrimental when distribution shifts occur, potentially leading to the acquisition of spurious knowledge and severe performance degradation. This raises a critical question: How should MLLMs and LLMs learn and utilize knowledge from ICE, discerning between factual information and statistical biases introduced by small sample sizes? When ICE and test data are from the same distribution, models should maximize knowledge extraction from ICE to efficiently acquire core knowledge. However, when distribution shifts are present, indiscriminate learning from ICE may be counterproductive. This provides a crucial research direction for improving MLLM generalization through ICL.

## 6. Conclusion

We introduce COUNTS, a comprehensive benchmark dataset designed to address the critical gap in evaluating and improving the OOD generalization capabilities of object detectors and MLLMs on fine-grained visual grounding tasks. By providing a large-scale dataset with diverse real-world distribution shifts and fine-grained annotations, COUNTS facilitates the development of more robust and reliable models for complex visual tasks. The proposed benchmarks,

O(OD)<sup>2</sup> and OODG, enable a thorough investigation of the factors influencing OOD generalization and offer insights for advancing research in this crucial area.

### **Acknowledgement**

This work was supported in part by China National Post-doctoral Program for Innovative Talents (BX20240203), Beijing Municipal Science and Technology Project (No. Z241100004224009), NSFC(No. 62425206, 62141607).

# COUNTS: Benchmarking Object Detectors and Multimodal Large Language Models under Distribution Shifts

## Supplementary Material

### A. More details about COUNTS

#### A.1. Selection of Domains

We identified 14 distinct domains: dim, painting, snow, sand, handmade, street, road, water, grass, indoor, mountain, sky, tree, and occlusion. These domains are prevalent in everyday visual experiences and are likely to exhibit distinct correlations with object occurrences. Importantly, while objects within the dataset samples are typically situated in the foreground, the identified domains often function as background elements or overarching image attributes. Consequently, we annotate domain labels at the image level, while providing bounding box annotations at the object level.

These domains are defined and described as follows.

- **Dim:** Images captured in suboptimal lighting conditions, often during dusk or dawn, resulting in objects blending with dimly lit backgrounds or obscured textures due to backlighting.
- **Painting:** Images where the primary objects are depicted within paintings rather than being real-world objects. This domain introduces potential discrepancies between the depicted objects and their real-world counterparts, as well as differences in background characteristics.
- **Snow:** Images featuring prominent snowy landscapes. Objects may be situated against bright, uniform snow backgrounds or partially covered by snow.
- **Handmade:** Images where the primary objects are hand-crafted, such as plastic or plush toys. These objects may differ in appearance from their real-world counterparts.
- **Street:** Images captured in street settings, typically characterized by outdoor, less open environments.
- **Road:** Images with road backgrounds, encompassing urban roads and highways. Compared to the "street" domain, "road" scenes predominantly feature major thoroughfares and highways, resulting in more open environments.
- **Water:** Images primarily featuring water surfaces or underwater scenes. Objects may be partially submerged or reflected in the water.
- **Grass:** Images with grassy backgrounds, primarily covered in low-lying vegetation, often appearing yellow or green. Objects may be partially obscured by vegetation.
- **Indoor:** Images captured in indoor environments, such as residences, stadiums, or exhibition halls. These scenes may exhibit specific lighting conditions and object states (e.g., objects displayed in showcases).

- **Mountain:** Images taken in mountainous regions, potentially featuring variations in viewing angles and exposed rock formations as backgrounds.
- **Sky:** Images with prominent sky backgrounds. Objects may be located at a distance from the camera or captured from a low-angle perspective.
- **Tree:** Images featuring trees, forests, or other tall vegetation as backgrounds, often appearing green or dark green.
- **Occlusion:** Images where the primary objects are partially or fully occluded, such as in crowded scenes where people are obscured by others.

#### A.2. Statistics of COUNTS

We report detailed statistical information on COUNTS<sup>1</sup> in this section. The number of samples per domain is presented in Table 6 and the number of samples per category is presented in Table 7.

### B. More Experiment Details

#### B.1. Evaluated Object Detectors

In this section, we introduce the evaluated object detectors via our O(OD)<sup>2</sup> benchmark. YOLO[68] is a real-time object detection model known for its speed and efficiency, using a single neural network to predict bounding boxes and class probabilities directly from full images. YOLOv9[78] is the latest iteration of the YOLO series, featuring improved accuracy, speed, and architecture modifications for enhanced object detection performance. RetinaNet[48] is a one-stage object detector that addresses the class imbalance problem in object detection by introducing a focal loss function. DETR[7] is an object detection model that leverages transformers and bipartite matching to eliminate the need for hand-designed components like anchor boxes and non-maximum suppression. DINO[93] is a self-supervised learning method for object detection that utilizes a teacher-student framework and contrastive learning to learn robust object representations without manual labeling.

#### B.2. Training Details of Detectors

For YOLOv9, we employed the official YOLOv9 implementation, while other models were implemented using MMDetection. Unless otherwise specified, all detectors were initialized with pre-trained parameters on ImageNet-1k. All the training is conducted for 60 epochs with an

<sup>1</sup>The COUNTS dataset can be found at <https://huggingface.co/datasets/jianshengli/COUNTS>

Domain	Dim	Painting	Snow	Sand	Handmade	Street	Road	Water	Grass	Indoor	Mountain	Sky	Tree	Occlusion		All
Images	26181	4167	3321	1788	2150	22474	12637	8915	14620	82719	1452	16771	45573	4215		246983
Objects	130448	14369	15029	15022	7671	185883	96506	34804	81530	470915	7578	74513	314532	28932		1477732

Table 6. Statistics of domains in COUNTS.

Category	person	sculpture	building	bicycle	wheel	car	train	glasses	truck	football	dress	dog	drum	guitar	motorcycle
Objects	564546	2378	41036	10170	48787	44418	3129	7952	2794	275	8228	5191	4239	5039	4307
Category	sunglasses	suit	boat	bird	flowerpot	houseplant	horse	poster	goggles	food	trousers	chair	shorts	wineglass	bicyclehelmet
Objects	4834	19319	1714	4003	2782	3143	3211	2533	1356	13624	5649	59916	3853	3884	2519
Category	umbrella	sunhat	helmet	drink	handbag										
Objects	4027	923	5128	9034	1029										

Table 7. Statistics of categories in COUNTS.

initial learning rate of 0.001, decayed by a factor of 0.1 at epochs 20 and 34. A batch size of 32 and a weight decay of 0.0001 were used. All experiments were performed using 8 NVIDIA RTX 4090 GPUs.

### B.3. Prompts for OODG

We show our prompt for Visual Grounding without and with ICE in Table 8 and 9, respectively.

We show our prompt for Recognition and Localization in Table 10.

We show our prompt for Visual and Semantic Mapping in Table 11.

## C. More Experimental Results

We present the performance of various MLLMs on the OODG benchmark, including GPT-4o, GPT-4-turbo, Gemini-1.5-Flash, Gemini-1.5-Pro, and Claude-3-Opus. Table 12 and 13 detail the results for each model on the Visual Grounding task.

While GPT-4-turbo demonstrates slightly weaker zero-shot performance compared to GPT-4o, their performance becomes comparable when distribution shifts exist between ICE and test samples, suggesting minimal influence from ICE on GPT-4-turbo. Overall, Gemini-1.5-Pro exhibits marginally stronger generalization capabilities than Gemini-1.5-Flash, but both are significantly affected by ICL and experience notable performance degradation when distribution shifts are present between ICE and test samples. Claude-3-Opus, while demonstrating slightly weaker zero-shot performance compared to GPT-4 and Gemini-1.5, appears less susceptible to being misled by biased ICE during ICL. These findings highlight significant variations in the generalization capabilities of different MLLMs and their varying degrees of reliance on and susceptibility to ICL. This underscores the importance of further research into leveraging ICL to enhance MLLM generalization while mitigating the potential negative impacts of biased or misaligned ICE.

### C.1. Visual and Semantic Mapping

We introduce a more challenging experimental setting, termed Visual and Semantic Mapping, which aims to assess a model’s ability to align visual regions with corresponding semantic information. Specifically, the model is presented with a set of visual regions and semantic descriptions, and tasked with establishing cross-modal correspondences between these elements. For simplicity, we formulate this task as a ranking problem, wherein the model observes visual regions in a fixed order and is then asked to rank a sequence of semantic descriptions to match the observed visual order. The prompt format for this task is detailed in Table 14.

The findings from the Visual and Semantic Mapping experiments align with those from the Visual Grounding and Recognition and Localization tasks, namely that GPT-4 exhibits marginally stronger zero-shot grounding capabilities compared to Gemini. Furthermore, Gemini demonstrates a significantly higher degree of reliance on and utilization of ICE than GPT-4. Consequently, Gemini’s performance improves notably when presented with IID ICE, but its generalization and stability are more susceptible to adverse effects when biased ICE are encountered.

### C.2. Results of Visual Grounding with more ICE

In the main paper, we present the capabilities of MLLMs with 0, 1, and 2 in-context examples (ICE). Here, we further analyze their performance when provided with a larger number of ICE (e.g., 4 and 8). The results are shown in Table 16. The results indicate that increasing the number of ICE does not significantly enhance the generalization capabilities of MLLMs. The presence of more biased ICE does not appear to further degrade their performance.

### C.3. Comparison of Object Detectors in OOD and i.i.d. Scenarios

We summarize the results of existing detectors on COUNT, as shown in Figure 2. We find that the target detection accuracy of existing detectors in OOD scenarios is significantly

---

Question: What object is in the red box? <image>
Option: (A) {category 1}
(B) {category 2}
(C) {category 3}
(D) {category 4}
Please respond with the following format:
—BEGIN FORMAT TEMPLATE—
Answer Choice: [Your Answer Choice Here]
—END FORMAT TEMPLATE—
Do not deviate from the above format. Repeat the format template for the answer.

---

Table 8. The prompt for Visual Grounding without ICE.

---

Answer the final question according to the following examples.
Examples:
Question: What object is in the red box? <image>
Option:
(A) {category 1}
(B) {category 2}
(C) {category 3}
(D) {category 4}
Please respond with the following format:
—BEGIN FORMAT TEMPLATE—
Answer Choice: [Your Answer Choice Here]
—END FORMAT TEMPLATE—
Do not deviate from the above format. Repeat the format template for the answer.
Answer choice: {ground truth}
... (other examples)
Final Question: What object is in the red box? <image>
Option:
(A) {category 1}
(B) {category 2}
(C) {category 3}
(D) {category 4}
Please respond with the following format:
—BEGIN FORMAT TEMPLATE—
Answer Choice: [Your Answer Choice Here]
—END FORMAT TEMPLATE—
Do not deviate from the above format. Repeat the format template for the answer.

---

Table 9. The prompt for Visual Grounding with ICE.

lower than that in i.i.d. scenarios, indicating a large room 5, respectively.  
for improvement in the OOD generalization ability of existing detectors.

#### C.4. Showcases in OODG

To provide a more intuitive understanding, we present the showcases of Visual Grounding, Recognition and Localization, and Visual and Semantic Mapping in Figure 3, 4, and

---

Knowing that the dimensions of the input image are weight weight and height height, find all the objects of category 1 in the image and return the coordinates [X, Y, W, H] of the rectangular box in which they are located, where X, Y denote the horizontal coordinate and the vertical coordinate of the upper-left corner of the rectangular box, respectively. W, H denote the weight and the height of the rectangular box, respectively.

Please respond with the following format:

—BEGIN FORMAT TEMPLATE—

Box item: [the coordinates of the box]

—END FORMAT TEMPLATE—

Do not deviate from the above format. Repeat the format template for the answer.

---

Table 10. The prompt for Recognition and Localization.

---

Question: What object is in the blue box, red box, yellow box, and green box, respectively? <image>

Option:

(A) {category 1}  
(B) {category 2}  
(C) {category 3}  
(D) {category 4}

Please respond with the following format:

—BEGIN FORMAT TEMPLATE—

Answer Choice:

blue box:[Your Answer Choice Here]  
red box:[Your Answer Choice Here]  
yellow box:[Your Answer Choice Here]  
green box:[Your Answer Choice Here]

—END FORMAT TEMPLATE—

Do not deviate from the above format. Repeat the format template for the answer.

---

Table 11. The prompt for Visual and Semantic Mapping.

Table 12. Results of Visual Grounding of more models on *sky*, *occlusion*, and *grass*. The selection accuracy is reported. *S*, *M*, and *L* indicate small, medium, and large objects, respectively.

Setting	Model	ICE	Sky			Occlusion			Grass		
			S	M	L	S	M	L	S	M	L
1	GPT-4o	0	0.434	0.727	0.889	0.362	0.891	0.805	0.969	0.939	0.818
	GPT-4-turbo-2024-04-09	0	0.286	0.500	0.917	0.308	0.444	0.833	0.813	0.833	0.667
	Gemini-1.5-Flash	0	0.444	0.667	0.778	0.355	0.674	0.628	0.424	0.343	0.615
	Gemini-1.5-Pro	0	0.438	0.671	0.744	0.372	0.674	0.624	0.428	0.329	0.614
	Claude-3-opus-2024-02-29	0	0.000	0.286	1.000	0.111	0.571	0.222	0.286	0.429	0.429
	groundingLMM	0	0.333	0.667	1.000	0.387	0.714	0.444	0.667	0.818	0.818
2	Qwen	0	0.286	0.667	0.889	0.333	0.667	0.355	0.424	0.667	0.714
	GPT-4o	1	0.445	0.778	0.778	0.571	1.000	1.000	0.857	0.857	0.714
		2	0.445	0.667	0.778	0.143	0.857	1.000	0.857	0.857	0.571
	GPT-4-turbo-2024-04-09	1	0.482	0.803	0.819	0.608	1.000	1.000	0.937	0.924	0.772
		2	0.487	0.679	0.808	0.157	0.891	1.000	0.917	0.870	0.598
	Gemini-1.5-Flash	1	0.444	0.714	1.000	0.143	1.000	0.857	0.833	1.000	0.429
3		2	0.444	0.857	1.000	0.143	1.000	1.000	1.000	1.000	0.788
	Gemini-1.5-Pro	1	0.465	0.777	1.000	0.143	1.000	0.910	0.852	1.000	0.459
		2	0.458	0.862	1.000	0.148	1.000	1.000	1.000	1.000	0.837
	Claude-3-opus-2024-02-29	1	0.250	0.562	1.000	0.111	0.222	0.147	0.400	0.083	0.556
		2	0.400	0.765	0.846	0.750	0.444	0.333	0.467	0.353	0.308
	GPT-4o	1	0.143	0.357	0.857	0.357	0.786	0.929	0.929	0.643	0.571
4		2	0.429	0.556	0.492	0.385	1.000	0.929	0.786	0.571	0.500
	GPT-4-turbo-2024-04-09	1	0.146	0.382	0.909	0.369	0.830	0.940	1.000	0.680	0.597
		2	0.432	0.602	0.499	0.421	1.000	0.945	0.845	0.590	0.529
	Gemini-1.5-Flash	1	0.222	0.143	0.143	0.143	0.143	0.143	0.111	0.111	0.111
		2	0.000	0.000	0.222	0.143	0.143	0.143	0.133	0.133	0.122
	Gemini-1.5-Pro	1	0.238	0.154	0.151	0.156	0.145	0.148	0.121	0.116	0.111
5		2	0.000	0.000	0.237	0.145	0.153	0.148	0.143	0.142	0.130
	Claude-3-opus-2024-02-29	1	0.208	1.000	0.636	0.111	0.857	0.571	0.232	0.000	1.000
		2	0.222	0.778	0.333	0.429	0.714	0.714	0.571	0.143	1.000
	GPT-4o	1	0.133	0.286	1.000	0.429	0.857	0.857	0.714	0.714	0.571
		2	0.143	0.286	1.000	0.286	0.571	0.857	1.000	0.857	0.857
	GPT-4-turbo-2024-04-09	1	0.143	0.310	1.000	0.441	0.887	0.926	0.765	0.751	0.602
6		2	0.145	0.288	1.000	0.294	0.617	0.937	1.000	0.891	0.919
	Gemini-1.5-Flash	1	0.000	0.111	0.143	0.111	0.133	0.127	0.111	0.111	0.286
		2	0.111	0.111	0.143	0.111	0.137	0.111	0.143	0.143	0.143
	Gemini-1.5-Pro	1	0.000	0.120	0.145	0.112	0.144	0.136	0.117	0.112	0.313
		2	0.111	0.111	0.143	0.111	0.137	0.111	0.143	0.143	0.143
	Claude-3-opus-2024-02-29	1	0.111	0.833	0.722	0.208	0.714	0.429	0.208	0.667	1.000
7		2	0.208	0.611	0.333	0.571	1.000	0.200	0.232	0.143	1.000
	GPT-4o	4	0.286	0.500	0.917	0.308	0.444	0.833	0.813	0.833	0.667
		8	0.714	0.875	0.833	0.311	0.556	0.833	0.938	0.611	0.583
	GPT-4-turbo-2024-04-09	4	0.294	0.518	0.964	0.318	0.468	0.890	0.853	0.885	0.730
		8	0.727	0.938	0.846	0.329	0.587	0.857	0.966	0.661	0.614
	Gemini-1.5-Flash	4	0.500	0.875	0.888	0.534	0.473	0.500	0.889	0.875	0.500
8		8	0.467	0.889	0.875	0.690	0.544	0.812	0.844	0.833	0.833
	Gemini-1.5-Pro	4	0.546	0.962	0.911	0.559	0.515	0.541	0.969	0.959	0.509
		8	0.497	0.937	0.889	0.738	0.573	0.835	0.859	0.852	0.839
	Claude-3-opus-2024-02-29	4	0.143	0.172	0.917	0.308	0.444	0.833	0.813	0.833	0.667
		8	0.167	0.214	0.917	0.308	0.444	0.833	0.813	0.833	0.667

Table 13. Results of Visual Grounding of more models on *water*, *dim*, and *handmake*. The selection accuracy is reported.

Setting	Model	ICE	Water			Dim			Handmake			Overall
			S	M	L	S	M	L	S	M	L	
1	GPT-4o	0	0.554	0.797	0.860	0.626	0.727	0.737	0.353	0.595	0.535	0.701
	GPT-4-turbo-2024-04-09	0	0.375	0.556	0.750	0.333	0.588	0.769	0.133	0.352	0.462	0.567
	Gemini-1.5-Flash	0	0.533	0.783	0.858	0.347	0.716	0.570	0.333	0.608	0.575	0.570
	Gemini-1.5-Pro	0	0.554	0.766	0.883	0.351	0.730	0.593	0.325	0.617	0.578	0.572
	Claude-3-opus-2024-02-29	0	0.571	0.429	0.714	0.286	0.714	0.857	0.143	0.714	0.714	0.471
	groundingLMM	0	0.554	0.857	1.000	0.429	0.857	0.857	0.333	0.429	0.513	0.648
	Qwen	0	0.533	0.667	0.750	0.385	0.625	0.714	0.286	0.444	0.555	0.551
2	GPT-4o	1	0.143	0.429	1.000	0.333	0.778	0.750	0.000	0.680	1.000	0.673
		2	0.554	0.797	0.860	0.333	0.778	0.778	0.000	0.825	1.000	0.672
	GPT-4-turbo-2024-04-09	1	0.149	0.449	1.000	0.350	0.779	0.774	0.000	0.720	1.000	0.710
		2	0.562	0.810	0.900	0.338	0.843	0.835	0.000	0.860	1.000	0.699
	Gemini-1.5-Flash	1	0.286	0.857	1.000	0.222	1.000	0.889	0.000	0.637	1.000	0.684
		2	0.143	0.857	1.000	0.333	1.000	0.889	0.000	0.671	1.000	0.729
	Gemini-1.5-Pro	1	0.290	0.916	1.000	0.229	1.000	0.908	0.000	0.682	1.000	0.714
3	Claude-3-opus-2024-02-29	1	0.231	0.444	0.667	0.232	0.232	0.571	0.400	0.429	0.429	0.387
		2	0.077	0.333	0.583	0.167	0.214	0.917	0.250	0.333	0.583	0.451
	GPT-4o	1	0.143	0.429	0.786	0.222	0.722	0.667	0.000	0.889	1.000	0.605
		2	0.143	0.429	0.929	0.278	0.778	0.778	0.000	0.714	1.000	0.604
	GPT-4-turbo-2024-04-09	1	0.147	0.450	0.816	0.240	0.780	0.694	0.000	0.916	1.000	0.606
		2	0.145	0.448	0.987	0.299	0.789	0.847	0.000	0.778	1.000	0.639
	Gemini-1.5-Flash	1	0.286	0.714	0.857	0.111	0.444	0.444	0.000	0.571	1.000	0.322
4		2	0.286	0.714	0.857	0.222	0.444	0.444	0.000	0.571	1.000	0.328
	Gemini-1.5-Pro	1	0.286	0.773	0.858	0.116	0.461	0.452	0.000	0.593	1.000	0.327
		2	0.290	0.741	0.869	0.222	0.453	0.481	0.000	0.596	1.000	0.350
	Claude-3-opus-2024-02-29	1	0.222	0.429	0.857	0.111	0.000	0.857	0.429	0.208	1.000	0.485
		2	0.143	0.143	0.714	0.000	0.200	0.857	0.000	0.222	0.857	0.447
	GPT-4o	1	0.143	0.429	0.857	0.000	0.556	0.667	0.342	0.432	1.000	0.580
		2	0.143	0.429	0.857	0.111	0.667	0.778	0.000	0.424	1.000	0.595
5	GPT-4-turbo-2024-04-09	1	0.149	0.445	0.903	0.000	0.572	0.706	0.375	0.441	1.000	0.584
		2	0.150	0.449	0.921	0.115	0.698	0.832	0.000	0.433	1.000	0.596
	Gemini-1.5-Flash	1	0.143	0.857	0.857	0.111	0.222	0.222	0.000	0.714	1.000	0.309
		2	0.143	1.000	0.714	0.000	0.222	0.222	0.000	0.424	1.000	0.280
	Gemini-1.5-Pro	1	0.145	0.932	0.893	0.114	0.237	0.234	0.000	0.734	1.000	0.305
		2	0.143	1.000	0.714	0.000	0.222	0.222	0.000	0.424	1.000	0.280
	Claude-3-opus-2024-02-29	1	0.111	0.429	0.714	0.232	0.222	0.929	0.000	0.111	0.857	0.472
6		2	0.333	0.308	0.786	0.286	0.143	0.857	0.273	0.400	1.000	0.482
	GPT-4o	4	0.375	0.556	0.750	0.333	0.588	0.769	0.133	0.352	0.462	0.567
		8	0.313	0.778	0.750	0.143	0.800	0.923	0.266	0.412	0.625	0.621
	GPT-4-turbo-2024-04-09	4	0.380	0.606	0.761	0.340	0.643	0.811	0.140	0.374	0.480	0.581
		8	0.336	0.800	0.759	0.147	0.826	0.997	0.277	0.445	0.656	0.654
	Gemini-1.5-Flash	4	0.375	0.556	0.750	0.347	0.716	0.570	0.400	0.313	0.769	0.608
		8	0.313	0.778	0.750	0.347	0.716	0.570	0.467	0.353	0.462	0.652
7	Gemini-1.5-Pro	4	0.409	0.557	0.806	0.373	0.779	0.575	0.403	0.325	0.796	0.639
		8	0.319	0.848	0.818	0.357	0.739	0.591	0.478	0.373	0.464	0.667
	Claude-3-opus-2024-02-29	4	0.375	0.556	0.750	0.333	0.588	0.769	0.133	0.352	0.462	0.525
8		8	0.375	0.556	0.750	0.333	0.588	0.769	0.133	0.352	0.462	0.529

Table 14. Results of Visual and Semantic Mapping. Mapping accuracy is reported.

Setting	Model	ICE	Occlusion			Dim			Handmake			Overall
			S	M	L	S	M	L	S	M	L	
1	GPT-4o	0	0.390	0.978	0.831	0.682	0.790	0.765	0.376	0.615	0.577	0.667
	Gemini-1.5-Flash	0	0.382	0.735	0.670	0.361	0.765	0.608	0.356	0.644	0.610	0.570
2	GPT-4o	1	0.620	1.000	1.000	0.343	0.814	0.764	0.000	0.726	1.000	0.707
	Gemini-1.5-Flash	2	0.151	0.889	1.000	0.361	0.812	0.814	0.000	0.902	1.000	0.660
3	GPT-4o	1	0.154	1.000	0.859	0.244	1.000	0.971	0.000	0.698	1.000	0.668
	Gemini-1.5-Flash	2	0.132	1.000	1.000	0.343	1.000	0.832	0.000	0.618	1.000	0.664
4	GPT-4o	1	0.358	0.774	0.979	0.204	0.670	0.733	0.000	0.908	1.000	0.625
	Gemini-1.5-Flash	2	0.412	1.000	0.880	0.301	0.764	0.783	0.000	0.700	1.000	0.649
5	GPT-4o	1	0.130	0.131	0.155	0.122	0.450	0.418	0.000	0.547	1.000	0.328
	Gemini-1.5-Flash	2	0.151	0.131	0.146	0.230	0.467	0.458	0.000	0.601	1.000	0.354
4	GPT-4o	1	0.414	0.877	0.849	0.000	0.526	0.654	0.345	0.428	1.000	0.566
	Gemini-1.5-Flash	2	0.307	0.551	0.919	0.116	0.607	0.856	0.000	0.388	1.000	0.527
5	GPT-4o	1	0.101	0.143	0.118	0.106	0.237	0.221	0.000	0.718	1.000	0.294
	Gemini-1.5-Flash	2	0.100	0.127	0.101	0.000	0.227	0.218	0.000	0.417	1.000	0.243
5	GPT-4o	4	0.295	0.477	0.901	0.319	0.649	0.816	0.131	0.351	0.464	0.489
	Gemini-1.5-Flash	8	0.346	0.569	0.826	0.152	0.745	0.963	0.288	0.476	0.603	0.552
5	GPT-4o	4	0.565	0.428	0.506	0.328	0.777	0.623	0.437	0.330	0.800	0.533
	Gemini-1.5-Flash	8	0.653	0.552	0.749	0.369	0.689	0.552	0.431	0.350	0.490	0.537

Table 15. Results of Visual Grounding with more ICE. Selection accuracy is reported.

Setting	Model	ICE	Occlusion			Dim			Handmake			Overall
			S	M	L	S	M	L	S	M	L	
2	GPT-4o	4	0.423	0.571	1.000	0.333	0.778	0.750	0.000	0.750	1.000	0.623
	Gemini-1.5-Flash	8	0.423	0.423	1.000	0.333	0.778	0.778	0.000	0.825	1.000	0.618
3	GPT-4o	4	0.375	0.857	0.857	0.333	0.500	0.750	0.000	0.750	1.000	0.602
	Gemini-1.5-Flash	8	0.400	0.571	0.714	0.333	0.571	0.769	0.000	0.675	1.000	0.559
3	GPT-4o	4	0.385	0.714	1.000	0.222	0.722	0.667	0.000	0.875	1.000	0.621
	Gemini-1.5-Flash	8	0.571	0.827	0.936	0.222	0.722	0.667	0.000	0.750	1.000	0.633
4	GPT-4o	4	0.111	0.147	0.147	0.111	0.444	0.444	0.000	0.750	1.000	0.350
	Gemini-1.5-Flash	8	0.111	0.147	0.147	0.111	0.444	0.444	0.000	0.500	1.000	0.323
4	GPT-4o	4	0.514	0.857	0.857	0.000	0.667	0.667	0.133	0.350	0.429	0.497
	Gemini-1.5-Flash	8	0.525	0.936	0.750	0.000	0.667	0.667	0.133	0.350	0.500	0.503
4	GPT-4o	4	0.111	0.375	0.200	0.111	0.222	0.167	0.400	0.429	0.429	0.272
	Gemini-1.5-Flash	8	0.111	0.375	0.144	0.111	0.111	0.222	0.400	0.429	0.429	0.259

Table 16. Results of Recognition and Localization with more ICE. mAP is reported.

Setting	Model	ICE	Occlusion			Dim	Handmake			Overall		
			S	M	L		S	M	L			
2	GPT-4o	4	0.101	0.062	0.088	0.064	0.098	0.084	0.082	0.063	0.092	0.077
		8	0.091	0.045	0.098	0.065	0.089	0.067	0.097	0.056	0.096	0.082
	Gemini-1.5-Flash	4	0.098	0.050	0.092	0.062	0.098	0.081	0.054	0.035	0.082	0.075
		8	0.084	0.025	0.078	0.067	0.080	0.080	0.082	0.051	0.069	0.075
3	GPT-4o	4	0.027	0.000	0.019	0.000	0.000	0.043	0.000	0.009	0.016	0.013
		8	0.023	0.004	0.014	0.000	0.000	0.045	0.000	0.005	0.023	0.013
	Gemini-1.5-Flash	4	0.000	0.000	0.000	0.000	0.000	0.000	0.000	0.000	0.000	0.000
		8	0.000	0.000	0.000	0.000	0.000	0.000	0.000	0.000	0.000	0.000
4	GPT-4o	4	0.009	0.000	0.085	0.001	0.000	0.000	0.091	0.005	0.084	0.031
		8	0.021	0.004	0.018	0.006	0.000	0.006	0.033	0.050	0.020	0.010
	Gemini-1.5-Flash	4	0.104	0.060	0.012	0.003	0.009	0.000	0.050	0.024	0.004	0.022
		8	0.002	0.099	0.013	0.008	0.034	0.002	0.098	0.019	0.098	0.045

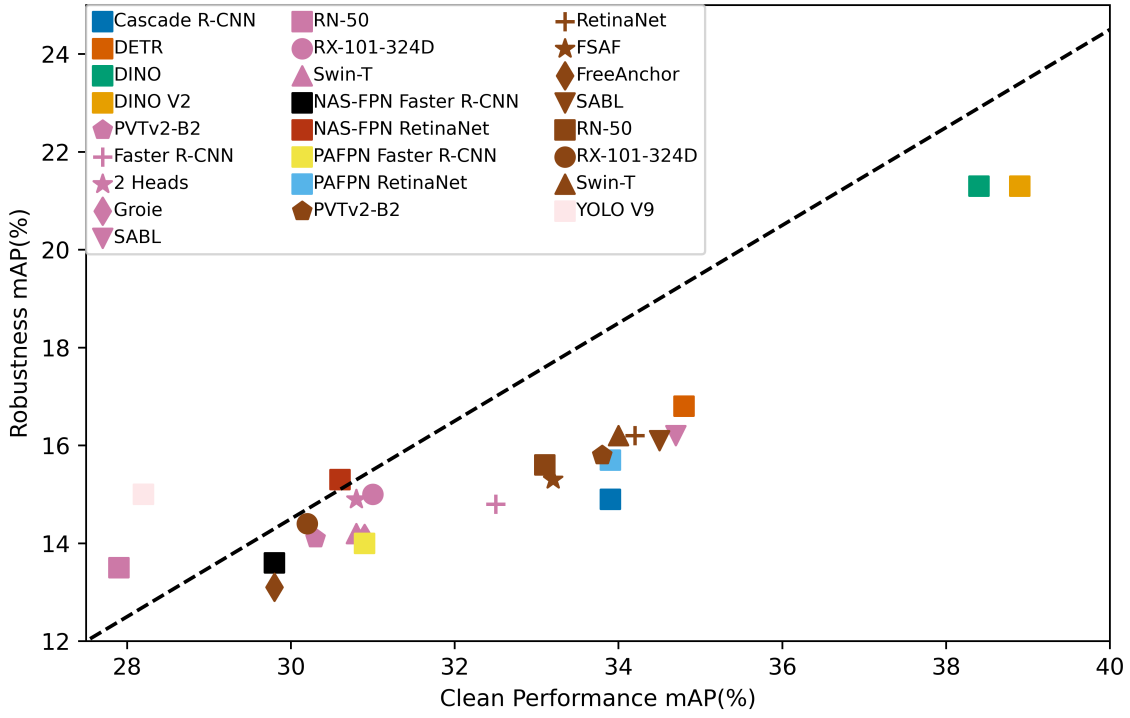


Figure 2. Comparison of current object detectors in OOD and i.i.d. scenarios.

## Prompt

Question: What object is in the red box? <image>

Option:

- (A) wheel
- (B) sunhat
- (C) train
- (D) guitar

Please respond with the following format:

—BEGIN FORMAT TEMPLATE—

Answer Choice: [Your Answer Choice Here]

Confidence Score: [Your Numerical Prediction Confidence Score Here From 0 To 1]

Reasoning: [Your Reasoning Behind This Answer Here]

—END FORMAT TEMPLATE—

Do not deviate from the above format. Repeat the format template for the answer.



**GPT-4o: Correct**

Answer Choice: [wheel]

Confidence Score: 0.95

Reasoning: The image shows a parade or event at night with decorated vehicles and bikes. A wheel is a common object found in such settings on cars and bicycles..

**Gemini-1.5-flash: Correct**

Answer Choice: [wheel]

Confidence Score: 0.8

Reasoning: Wheels are clearly visible on both the truck and the car in the image.

## Prompt

Question: What object is in the blue box, red boxrespectively? <image>

Option:

- (A) drink
- (B) person

Please respond with the following format:

—BEGIN FORMAT TEMPLATE—

Answer Choice:

blue box:[Your Answer Choice Here]

red box:[Your Answer Choice Here]

—END FORMAT TEMPLATE—

Do not deviate from the above format. Repeat the format template for the answer.



**GPT-4o:**

**Answer Choice:**

Bluebox:[person]

Redbox:[drink]

Confidence Score: 0.95

Reasoning: The image shows a person and the drink on the table.

**Gemini-1.5-flash:**

**Answer Choice:**

Bluebox:[person]

Redbox:[drink]

Confidence Score: 0.95

Reasoning: The image shows the person in the blue box and the bottle like drink in the redbox.

Figure 4. Example of Recognition and Localization.

## Prompt

Knowing that the dimensions of the input image are weight 448 and height 448, find all the objects of truck in the image and return the coordinates [X, Y, W, H] of the rectangular box in which they are located, where X, Y denote the horizontal coordinate and the vertical coordinate of the upper-left corner of the rectangular box, respectively. W, H denote the weight and the height of the rectangular box, respectively.

Please respond with the following format:

—BEGIN FORMAT TEMPLATE—

Box item: [the coordinates of the box]

—END FORMAT TEMPLATE—

Do not deviate from the above format. Repeat the format template for the answer.



**GPT-4o:**

Answer Choice: [419, 32, 28, 19]

**Gemini-1.5-flash:**

Answer Choice: [400, 30, 25, 20]

Figure 5. Example of Visual and Semantic Mapping.

## D. Limitations

The proposed OODG benchmark presented in this work focuses on evaluating the OOD generalization capabilities of MLLMs with respect to the distribution shift between ICE and test samples. However, it does not explicitly address potential distribution shifts that may arise between the supervised fine-tuning (SFT) data and test samples. Future work could leverage COUNTS to conduct SFT on MLLMs and investigate the impact of distribution shifts occurring during the SFT phase, as well as potential mitigation strategies.

## E. Broader Impact

The broader impact of this work is significant for both the research community and real-world applications. COUNTS, the introduced dataset, provides a valuable resource for advancing research in OOD generalization, a critical area for deploying robust and reliable machine learning models in real-world scenarios. By focusing on fine-grained object detection and grounding tasks, COUNTS enables the development of models that can accurately perceive and understand visual information even in novel and challenging environments.

Furthermore, the proposed benchmarks, O(OD)<sup>2</sup> and OODG, establish standardized evaluation protocols for assessing the OOD generalization capabilities of object detectors and MLLMs, respectively. These benchmarks will serve as valuable tools for researchers and practitioners to gauge the robustness and trustworthiness of their models, ultimately leading to the development of more reliable and adaptable AI systems.

The insights gained from this research can have far-reaching implications across various domains, including autonomous vehicles, robotics, surveillance, and content moderation, where the ability to accurately detect and ground objects under diverse and unpredictable conditions is paramount. Ultimately, this work contributes to the development of AI systems that are more aligned with human visual perception and understanding, thereby increasing their potential for safe and beneficial deployment in real-world applications.

## References

- [1] Jean-Baptiste Alayrac, Jeff Donahue, Pauline Luc, Antoine Miech, Iain Barr, and et al. Flamingo: a visual language model for few-shot learning. *Advances in Neural Information Processing Systems*, 35:23716–23736, 2022.
- [2] Anas Awadalla, Irena Gao, Josh Gardner, Jack Hessel, Yusuf Hanafy, Wanrong Zhu, Kalyani Marathe, Yonatan Bitton, Samir Gadre, Shiori Sagawa, et al. Openflamingo: An open-source framework for training large autoregressive vision-language models. *arXiv preprint arXiv:2308.01390*, 2023.
- [3] Jinze Bai, Shuai Bai, Shusheng Yang, Shijie Wang, Sinan Tan, and et al. Qwen-vl: A frontier large vision-language model with versatile abilities. *arXiv preprint arXiv:2308.12966*, 2023.
- [4] Shuai Bai, Shusheng Yang, Jinze Bai, Peng Wang, Xingxuan Zhang, Junyang Lin, Xinggang Wang, Chang Zhou, and Jingren Zhou. Touchstone: Evaluating vision-language models by language models. *arXiv preprint arXiv:2308.16890*, 2023.
- [5] Zhaowei Cai and Nuno Vasconcelos. Cascade r-cnn: High quality object detection and instance segmentation. *IEEE transactions on pattern analysis and machine intelligence*, 43(5):1483–1498, 2019.
- [6] Nicolas Carion, Francisco Massa, Gabriel Synnaeve, Nicolas Usunier, Alexander Kirillov, and Sergey Zagoruyko. End-to-end object detection with transformers. *CoRR*, abs/2005.12872, 2020.
- [7] Nicolas Carion, Francisco Massa, Gabriel Synnaeve, Nicolas Usunier, Alexander Kirillov, and Sergey Zagoruyko. End-to-end object detection with transformers. In *European conference on computer vision*, pages 213–229. Springer, 2020.
- [8] Mathilde Caron, Hugo Touvron, Ishan Misra, Hervé Jégou, Julien Mairal, Piotr Bojanowski, and Armand Joulin. Emerging properties in self-supervised vision transformers. *CoRR*, abs/2104.14294, 2021.
- [9] Xinlei Chen, Haoqi Fan, Ross Girshick, and Kaiming He. Improved baselines with momentum contrastive learning. *arXiv preprint arXiv:2003.04297*, 2020.
- [10] Yen-Chun Chen, Linjie Li, Licheng Yu, Ahmed El Kholy, Faisal Ahmed, Zhe Gan, Yu Cheng, and Jingjing Liu. Uniter: Universal image-text representation learning. In *European conference on computer vision*, pages 104–120. Springer, 2020.
- [11] Marius Cordts, Mohamed Omran, Sebastian Ramos, Timo Rehfeld, Markus Enzweiler, Rodrigo Benenson, Uwe Franke, Stefan Roth, and Bernt Schiele. The cityscapes dataset for semantic urban scene understanding. In *2016 IEEE Conference on Computer Vision and Pattern Recognition (CVPR)*, pages 3213–3223, 2016.
- [12] Chenhang Cui, Yiyang Zhou, Xinyu Yang, Shirley Wu, Linjun Zhang, James Zou, and Huaxiu Yao. Holistic analysis of hallucination in gpt-4v (ision): Bias and interference challenges. *arXiv preprint arXiv:2311.03287*, 2023.
- [13] Mark Everingham, SM Ali Eslami, Luc Van Gool, Christopher KI Williams, John Winn, and Andrew Zisserman. The pascal visual object classes challenge: A retrospective. *International journal of computer vision*, 111:98–136, 2015.
- [14] Chen Fang, Ye Xu, and Daniel N. Rockmore. Unbiased metric learning: On the utilization of multiple datasets and web images for softening bias. In *2013 IEEE International Conference on Computer Vision*, pages 1657–1664, 2013.
- [15] Peng Gao, Jiaming Han, Renrui Zhang, Ziwei Lin, Shijie Geng, Aojun Zhou, Wei Zhang, Pan Lu, Conghui He, Xiangyu Yue, et al. Llama-adapter v2: Parameter-efficient visual instruction model. *arXiv preprint arXiv:2304.15010*, 2023.
- [16] Andreas Geiger, Philip Lenz, and Raquel Urtasun. Are we ready for autonomous driving? the kitti vision benchmark suite. In *2012 IEEE Conference on Computer Vision and Pattern Recognition*, pages 3354–3361, 2012.
- [17] Golnaz Ghiasi, Tsung-Yi Lin, and Quoc V Le. Nas-fpn: Learning scalable feature pyramid architecture for object detection. In *Proceedings of the IEEE/CVF conference on computer vision and pattern recognition*, pages 7036–7045, 2019.
- [18] Ross Girshick. Fast r-cnn. In *Proceedings of the IEEE international conference on computer vision*, pages 1440–1448, 2015.
- [19] Ross Girshick, Jeff Donahue, Trevor Darrell, and Jitendra Malik. Rich feature hierarchies for accurate object detection and semantic segmentation. In *Proceedings of the IEEE conference on computer vision and pattern recognition*, pages 580–587, 2014.
- [20] Yash Goyal, Tejas Khot, Douglas Summers-Stay, Dhruv Batra, and Devi Parikh. Making the v in vqa matter: Elevating the role of image understanding in visual question answering. In *Proceedings of the IEEE conference on computer vision and pattern recognition*, pages 6904–6913, 2017.
- [21] Ishaan Gulrajani and David Lopez-Paz. In search of lost domain generalization. *arXiv preprint arXiv:2007.01434*, 2020.
- [22] Zhongyi Han, Guanglin Zhou, Rundong He, Jindong Wang, Xing Xie, Tailin Wu, Yilong Yin, Salman Khan, Lina Yao, Tongliang Liu, et al. How well does gpt-4v (ision) adapt to distribution shifts? a preliminary investigation. *arXiv preprint arXiv:2312.07424*, 2023.
- [23] Kaiming He, Xiangyu Zhang, Shaoqing Ren, and Jian Sun. Deep residual learning for image recognition. In *Proceedings of the IEEE conference on computer vision and pattern recognition*, pages 770–778, 2016.
- [24] Kaiming He, Georgia Gkioxari, Piotr Dollár, and Ross Girshick. Mask r-cnn. In *Proceedings of the IEEE international conference on computer vision*, pages 2961–2969, 2017.
- [25] Zhenwei He and Lei Zhang. Multi-adversarial faster-rcnn for unrestricted object detection. In *2019 IEEE/CVF International Conference on Computer Vision (ICCV)*, pages 6667–6676, 2019.
- [26] Dan Hendrycks and Thomas Dietterich. Benchmarking neural network robustness to common corruptions and perturbations. *arXiv preprint arXiv:1903.12261*, 2019.

- [27] Dan Hendrycks, Steven Basart, Norman Mu, Saurav Kadavath, Frank Wang, Evan Dorundo, Rahul Desai, Tyler Zhu, Samyak Parajuli, Mike Guo, et al. The many faces of robustness: A critical analysis of out-of-distribution generalization. In *Proceedings of the IEEE/CVF international conference on computer vision*, pages 8340–8349, 2021.
- [28] Dan Hendrycks, Kevin Zhao, Steven Basart, Jacob Steinhardt, and Dawn Song. Natural adversarial examples. In *Proceedings of the IEEE/CVF conference on computer vision and pattern recognition*, pages 15262–15271, 2021.
- [29] Yupan Huang, Zaiqiao Meng, Fangyu Liu, Yixuan Su, Nigel Collier, and Yutong Lu. Sparkles: Unlocking chats across multiple images for multimodal instruction-following models. *arXiv preprint arXiv:2308.16463*, 2023.
- [30] Drew A Hudson and Christopher D Manning. Gqa: A new dataset for real-world visual reasoning and compositional question answering. In *Proceedings of the IEEE/CVF conference on computer vision and pattern recognition*, pages 6700–6709, 2019.
- [31] Naoto Inoue, Ryosuke Furuta, Toshihiko Yamasaki, and Kiyoharu Aizawa. Cross-domain weakly-supervised object detection through progressive domain adaptation. In *Proceedings of the IEEE Conference on Computer Vision and Pattern Recognition (CVPR)*, 2018.
- [32] Yixing Jiang, Jeremy Irvin, Ji Hun Wang, Muhammad Ahmed Chaudhry, Jonathan H Chen, and Andrew Y Ng. Many-shot in-context learning in multimodal foundation models. *arXiv preprint arXiv:2405.09798*, 2024.
- [33] Matthew Johnson-Roberson, Charles Barto, Rounak Mehta, Sharath Nittur Sridhar, Karl Rosaen, and Ram Vasudevan. Driving in the matrix: Can virtual worlds replace human-generated annotations for real world tasks? In *2017 IEEE International Conference on Robotics and Automation (ICRA)*, pages 746–753, 2017.
- [34] Sahar Kazemzadeh, Vicente Ordonez, Mark Matten, and Tamara Berg. Referitgame: Referring to objects in photographs of natural scenes. In *Proceedings of the 2014 conference on empirical methods in natural language processing (EMNLP)*, pages 787–798, 2014.
- [35] Mehran Khodabandeh, Arash Vahdat, Mani Ranjbar, and William Macready. A robust learning approach to domain adaptive object detection. In *2019 IEEE/CVF International Conference on Computer Vision (ICCV)*, pages 480–490, 2019.
- [36] Pang Wei Koh, Shiori Sagawa, Henrik Marklund, Sang Michael Xie, Marvin Zhang, Akshay Balsubramani, Weihua Hu, Michihiro Yasunaga, Richard Lanas Phillips, Irena Gao, et al. Wilds: A benchmark of in-the-wild distribution shifts. In *International conference on machine learning*, pages 5637–5664. PMLR, 2021.
- [37] Ranjay Krishna, Yuke Zhu, Oliver Groth, Justin Johnson, Kenji Hata, Joshua Kravitz, Stephanie Chen, Yannis Kalantidis, Li-Jia Li, David A Shamma, et al. Visual genome: Connecting language and vision using crowdsourced dense image annotations. *International journal of computer vision*, 123:32–73, 2017.
- [38] Alina Kuznetsova, Hassan Rom, Neil Alldrin, Jasper Uijlings, Ivan Krasin, Jordi Pont-Tuset, Shahab Kamali, Stefan Popov, Matteo Malloci, Alexander Kolesnikov, et al. The open images dataset v4: Unified image classification, object detection, and visual relationship detection at scale. *International journal of computer vision*, 128(7):1956–1981, 2020.
- [39] Yann LeCun, Léon Bottou, Yoshua Bengio, and Patrick Haffner. Gradient-based learning applied to document recognition. *Proceedings of the IEEE*, 86(11):2278–2324, 1998.
- [40] Bohao Li, Rui Wang, Guangzhi Wang, Yuying Ge, Yixiao Ge, and Ying Shan. Seed-bench: Benchmarking multi-modal llms with generative comprehension. *arXiv preprint arXiv:2307.16125*, 2023.
- [41] Bo Li, Yuanhan Zhang, Liangyu Chen, Jinghao Wang, Fanyi Pu, Jingkang Yang, Chunyuan Li, and Ziwei Liu. Mimic-it: Multi-modal in-context instruction tuning. *arXiv preprint arXiv:2306.05425*, 2023.
- [42] Da Li, Yongxin Yang, Yi-Zhe Song, and Timothy M. Hospedales. Deeper, broader and artier domain generalization. In *2017 IEEE International Conference on Computer Vision (ICCV)*, pages 5543–5551, 2017.
- [43] Da Li, Yongxin Yang, Yi-Zhe Song, and Timothy M Hospedales. Deeper, broader and artier domain generalization. In *Proceedings of the IEEE international conference on computer vision*, pages 5542–5550, 2017.
- [44] Xiuju Li, Xi Yin, Chunyuan Li, Pengchuan Zhang, Xiaowei Hu, Lei Zhang, Lijuan Wang, Houdong Hu, Li Dong, Furu Wei, et al. Oscar: Object-semantics aligned pre-training for vision-language tasks. In *Computer Vision–ECCV 2020: 16th European Conference, Glasgow, UK, August 23–28, 2020, Proceedings, Part XXX 16*, pages 121–137. Springer, 2020.
- [45] Chuang Lin, Zehuan Yuan, Sicheng Zhao, Peize Sun, Changhu Wang, and Jianfei Cai. Domain-invariant disentangled network for generalizable object detection. In *2021 IEEE/CVF International Conference on Computer Vision (ICCV)*, pages 8751–8760, 2021.
- [46] Tsung-Yi Lin, Michael Maire, Serge Belongie, James Hays, Pietro Perona, Deva Ramanan, Piotr Dollár, and C Lawrence Zitnick. Microsoft coco: Common objects in context. In *Computer Vision–ECCV 2014: 13th European Conference, Zurich, Switzerland, September 6–12, 2014, Proceedings, Part V 13*, pages 740–755. Springer, 2014.
- [47] Tsung-Yi Lin, Piotr Dollár, Ross Girshick, Kaiming He, Bharath Hariharan, and Serge Belongie. Feature pyramid networks for object detection. In *Proceedings of the IEEE conference on computer vision and pattern recognition*, pages 2117–2125, 2017.
- [48] Tsung-Yi Lin, Priya Goyal, Ross Girshick, Kaiming He, and Piotr Dollár. Focal loss for dense object detection. In *Proceedings of the IEEE international conference on computer vision*, pages 2980–2988, 2017.
- [49] Shu Liu, Lu Qi, Haifang Qin, Jianping Shi, and Jiaya Jia. Path aggregation network for instance segmentation. In *Proceedings of the IEEE conference on computer vision and pattern recognition*, pages 8759–8768, 2018.
- [50] Wei Liu, Dragomir Anguelov, Dumitru Erhan, Christian Szegedy, Scott Reed, Cheng-Yang Fu, and Alexander C

- Berg. Ssd: Single shot multibox detector. In *Computer Vision–ECCV 2016: 14th European Conference, Amsterdam, The Netherlands, October 11–14, 2016, Proceedings, Part I* 14, pages 21–37. Springer, 2016.
- [51] Yuan Liu, Haodong Duan, Yuanhan Zhang, Bo Li, Songyang Zhang, Wangbo Zhao, Yike Yuan, Jiaqi Wang, Conghui He, Ziwei Liu, et al. Mmbench: Is your multi-modal model an all-around player? *arXiv preprint arXiv:2307.06281*, 2023.
- [52] Ze Liu, Yutong Lin, Yue Cao, Han Hu, Yixuan Wei, Zheng Zhang, Stephen Lin, and Baining Guo. Swin transformer: Hierarchical vision transformer using shifted windows. In *Proceedings of the IEEE/CVF international conference on computer vision*, pages 10012–10022, 2021.
- [53] Pan Lu, Hritik Bansal, Tony Xia, Jiacheng Liu, Chun-yuan Li, Hannaneh Hajishirzi, Hao Cheng, Kai-Wei Chang, Michel Galley, and Jianfeng Gao. Mathvista: Evaluating mathematical reasoning of foundation models in visual contexts. *arXiv preprint arXiv:2310.02255*, 2023.
- [54] Xiaofeng Mao, Yuefeng Chen, Yao Zhu, Da Chen, Hang Su, Rong Zhang, and Hui Xue. Coco-o: A benchmark for object detectors under natural distribution shifts. In *2023 IEEE/CVF International Conference on Computer Vision (ICCV)*, pages 6316–6327, 2023.
- [55] Xiaofeng Mao, Yuefeng Chen, Yao Zhu, Da Chen, Hang Su, Rong Zhang, and Hui Xue. Coco-o: A benchmark for object detectors under natural distribution shifts. In *Proceedings of the IEEE/CVF International Conference on Computer Vision*, pages 6339–6350, 2023.
- [56] Kenneth Marino, Mohammad Rastegari, Ali Farhadi, and Roozbeh Mottaghi. Ok-vqa: A visual question answering benchmark requiring external knowledge. In *Proceedings of the IEEE/cvf conference on computer vision and pattern recognition*, pages 3195–3204, 2019.
- [57] Grégoire Mialon, Clémentine Fourrier, Craig Swift, Thomas Wolf, Yann LeCun, and Thomas Scialom. Gaia: a benchmark for general ai assistants. *arXiv preprint arXiv:2311.12983*, 2023.
- [58] Claudio Michaelis, Benjamin Mitzkus, Robert Geirhos, Evgenia Rusak, Oliver Bringmann, Alexander S. Ecker, Matthias Bethge, and Wieland Brendel. Benchmarking robustness in object detection: Autonomous driving when winter is coming. *CoRR*, abs/1907.07484, 2019.
- [59] Claudio Michaelis, Benjamin Mitzkus, Robert Geirhos, Evgenia Rusak, Oliver Bringmann, Alexander S Ecker, Matthias Bethge, and Wieland Brendel. Benchmarking robustness in object detection: Autonomous driving when winter is coming. *arXiv preprint arXiv:1907.07484*, 2019.
- [60] Masoud Monajatipoor, Liunian Harold Li, Mozhdeh Rouhsedaghat, Lin F Yang, and Kai-Wei Chang. Metavl: Transferring in-context learning ability from language models to vision-language models. *arXiv preprint arXiv:2306.01311*, 2023.
- [61] OpenAI. Gpt-4 technical report, 2023.
- [62] Maxime Oquab, Timothée Darcet, Théo Moutakanni, Huy Vo, Marc Szafraniec, Vasil Khalidov, Pierre Fernandez, Daniel Haziza, Francisco Massa, Alaaeldin El-Nouby, Mahmoud Assran, Nicolas Ballas, Wojciech Galuba, Russell Howes, Po-Yao Huang, Shang-Wen Li, Ishan Misra, Michael Rabbat, Vasu Sharma, Gabriel Synnaeve, Hu Xu, Hervé Jegou, Julien Mairal, Patrick Labatut, Armand Joulin, and Piotr Bojanowski. Dinov2: Learning robust visual features without supervision. *arXiv preprint arXiv:2304.07193*, 2023.
- [63] Xingchao Peng, Qinxun Bai, Xide Xia, Zijun Huang, Kate Saenko, and Bo Wang. Moment matching for multi-source domain adaptation. In *2019 IEEE/CVF International Conference on Computer Vision (ICCV)*, pages 1406–1415, 2019.
- [64] Bryan A Plummer, Liwei Wang, Chris M Cervantes, Juan C Caicedo, Julia Hockenmaier, and Svetlana Lazebnik. Flickr30k entities: Collecting region-to-phrase correspondences for richer image-to-sentence models. In *Proceedings of the IEEE international conference on computer vision*, pages 2641–2649, 2015.
- [65] Alec Radford, Jong Wook Kim, Chris Hallacy, Aditya Ramesh, Gabriel Goh, Sandhini Agarwal, Girish Sastry, Amanda Askell, Pamela Mishkin, Jack Clark, et al. Learning transferable visual models from natural language supervision. In *International conference on machine learning*, pages 8748–8763. PMLR, 2021.
- [66] Hanoona Rasheed, Muhammad Maaz, Sahal Shaji, Abdelrahman Shaker, Salman Khan, Hisham Cholakkal, Rao M Anwer, Eric Xing, Ming-Hsuan Yang, and Fahad S Khan. Glamm: Pixel grounding large multimodal model. *arXiv preprint arXiv:2311.03356*, 2023.
- [67] Hanoona Rasheed, Muhammad Maaz, Sahal Shaji, Abdelrahman Shaker, Salman Khan, Hisham Cholakkal, Rao M Anwer, Eric Xing, Ming-Hsuan Yang, and Fahad S Khan. Glamm: Pixel grounding large multimodal model. In *Proceedings of the IEEE/CVF Conference on Computer Vision and Pattern Recognition*, pages 13009–13018, 2024.
- [68] Joseph Redmon, Santosh Divvala, Ross Girshick, and Ali Farhadi. You only look once: Unified, real-time object detection. In *Proceedings of the IEEE conference on computer vision and pattern recognition*, pages 779–788, 2016.
- [69] Shaoqing Ren, Kaiming He, Ross Girshick, and Jian Sun. Faster r-cnn: Towards real-time object detection with region proposal networks. *Advances in neural information processing systems*, 28, 2015.
- [70] Tal Ridnik, Emanuel Ben-Baruch, Asaf Noy, and Lih Zelnik-Manor. Imagenet-21k pretraining for the masses. *arXiv preprint arXiv:2104.10972*, 2021.
- [71] Leonardo Rossi, Akbar Karimi, and Andrea Prati. A novel region of interest extraction layer for instance segmentation. In *2020 25th international conference on pattern recognition (ICPR)*, pages 2203–2209. IEEE, 2021.
- [72] Hao Tan and Mohit Bansal. Lxmert: Learning cross-modality encoder representations from transformers. *arXiv preprint arXiv:1908.07490*, 2019.
- [73] Mingxing Tan, Ruoming Pang, and Quoc V Le. Efficientdet: Scalable and efficient object detection. In *Proceedings of the IEEE/CVF conference on computer vision and pattern recognition*, pages 10781–10790, 2020.

- [74] Gemini Team, Rohan Anil, Sebastian Borgeaud, Yonghui Wu, Jean-Baptiste Alayrac, and et al. Gemini: a family of highly capable multimodal models. *arXiv preprint arXiv:2312.11805*, 2023.
- [75] Zhi Tian, Xiangxiang Chu, Xiaoming Wang, Xiaolin Wei, and Chunhua Shen. Fully convolutional one-stage 3d object detection on lidar range images. *Advances in Neural Information Processing Systems*, 35:34899–34911, 2022.
- [76] Ashish Vaswani, Noam Shazeer, Niki Parmar, Jakob Uszkoreit, Llion Jones, Aidan N Gomez, Łukasz Kaiser, and Illia Polosukhin. Attention is all you need. *Advances in neural information processing systems*, 30, 2017.
- [77] Hemanth Venkateswara, Jose Eusebio, Shayok Chakraborty, and Sethuraman Panchanathan. Deep hashing network for unsupervised domain adaptation. In *2017 IEEE Conference on Computer Vision and Pattern Recognition (CVPR)*, pages 5385–5394, 2017.
- [78] Chien-Yao Wang, I-Hau Yeh, and Hong-Yuan Mark Liao. Yolov9: Learning what you want to learn using programmable gradient information. *arXiv preprint arXiv:2402.13616*, 2024.
- [79] Jiaqi Wang, Wenwei Zhang, Yuhang Cao, Kai Chen, Jiangmiao Pang, Tao Gong, Jianping Shi, Chen Change Loy, and Dahua Lin. Side-aware boundary localization for more precise object detection. In *Computer Vision–ECCV 2020: 16th European Conference, Glasgow, UK, August 23–28, 2020, Proceedings, Part IV 16*, pages 403–419. Springer, 2020.
- [80] Jindong Wang, Cuiling Lan, Chang Liu, Yidong Ouyang, Tao Qin, Wang Lu, Yiqiang Chen, Wenjun Zeng, and S Yu Philip. Generalizing to unseen domains: A survey on domain generalization. *IEEE transactions on knowledge and data engineering*, 35(8):8052–8072, 2022.
- [81] Peng Wang, Shuai Bai, Sinan Tan, Shijie Wang, Zhihao Fan, Jinze Bai, Keqin Chen, Xuejing Liu, Jialin Wang, Wenbin Ge, et al. Qwen2-vl: Enhancing vision-language model’s perception of the world at any resolution. *arXiv preprint arXiv:2409.12191*, 2024.
- [82] Wenhui Wang, Enze Xie, Xiang Li, Deng-Ping Fan, Kaitao Song, Ding Liang, Tong Lu, Ping Luo, and Ling Shao. Pvt v2: Improved baselines with pyramid vision transformer. *Computational Visual Media*, 8(3):415–424, 2022.
- [83] Ross Wightman, Hugo Touvron, and Hervé Jégou. Resnet strikes back: An improved training procedure in timm. *arXiv preprint arXiv:2110.00476*, 2021.
- [84] Yue Wu, Yinpeng Chen, Lu Yuan, Zicheng Liu, Lijuan Wang, Hongzhi Li, and Yun Fu. Rethinking classification and localization for object detection. In *Proceedings of the IEEE/CVF conference on computer vision and pattern recognition*, pages 10186–10195, 2020.
- [85] Saining Xie, Ross Girshick, Piotr Dollar, Zhuowen Tu, and Kaiming He. Aggregated residual transformations for deep neural networks. In *Proceedings of the IEEE conference on computer vision and pattern recognition*, pages 1492–1500, 2017.
- [86] Peng Xu, Wenqi Shao, Kaipeng Zhang, Peng Gao, Shuo Liu, Meng Lei, Fanqing Meng, Siyuan Huang, Yu Qiao, and Ping Luo. Lvlm-ehub: A comprehensive evaluation benchmark for large vision-language models. *arXiv preprint arXiv:2306.09265*, 2023.
- [87] Zhengyuan Yang, Linjie Li, Kevin Lin, Jianfeng Wang, Chung-Ching Lin, and et al. The dawn of lmms: Preliminary explorations with gpt-4v (ision). *arXiv preprint arXiv:2309.17421*, 9(1):1, 2023.
- [88] Fisher Yu, Haofeng Chen, Xin Wang, Wenqi Xian, Yingying Chen, Fangchen Liu, Vashisht Madhavan, and Trevor Darrell. Bdd100k: A diverse driving dataset for heterogeneous multitask learning. In *Proceedings of the IEEE/CVF Conference on Computer Vision and Pattern Recognition (CVPR)*, 2020.
- [89] Han Yu, Xingxuan Zhang, Renzhe Xu, Jiashuo Liu, Yue He, and Peng Cui. Rethinking the evaluation protocol of domain generalization. *arXiv preprint arXiv:2305.15253*, 2023.
- [90] Licheng Yu, Patrick Poirson, Shan Yang, Alexander C Berg, and Tamara L Berg. Modeling context in referring expressions. In *Computer Vision–ECCV 2016: 14th European Conference, Amsterdam, The Netherlands, October 11–14, 2016, Proceedings, Part II 14*, pages 69–85. Springer, 2016.
- [91] Weihao Yu, Zhengyuan Yang, Linjie Li, Jianfeng Wang, Kevin Lin, Zicheng Liu, Xinchao Wang, and Lijuan Wang. Mm-vet: Evaluating large multimodal models for integrated capabilities. *arXiv preprint arXiv:2308.02490*, 2023.
- [92] Xiang Yue, Yuansheng Ni, Kai Zhang, Tianyu Zheng, Ruqi Liu, Ge Zhang, Samuel Stevens, Dongfu Jiang, Weiming Ren, Yuxuan Sun, et al. Mmmu: A massive multidiscipline multimodal understanding and reasoning benchmark for expert agi. *arXiv preprint arXiv:2311.16502*, 2023.
- [93] Hao Zhang, Feng Li, Shilong Liu, Lei Zhang, Hang Su, Jun Zhu, Lionel M Ni, and Heung-Yeung Shum. Dino: Detr with improved denoising anchor boxes for end-to-end object detection. *arXiv preprint arXiv:2203.03605*, 2022.
- [94] Pengchuan Zhang, Xiujun Li, Xiaowei Hu, Jianwei Yang, Lei Zhang, Lijuan Wang, Yejin Choi, and Jianfeng Gao. Vinvl: Revisiting visual representations in vision-language models. In *Proceedings of the IEEE/CVF conference on computer vision and pattern recognition*, pages 5579–5588, 2021.
- [95] Xiaosong Zhang, Fang Wan, Chang Liu, Rongrong Ji, and Qixiang Ye. Freeanchor: Learning to match anchors for visual object detection. In *Advances in Neural Information Processing Systems*, pages 147–155, 2019.
- [96] Xingxuan Zhang, Yue He, Renzhe Xu, Han Yu, Zheyuan Shen, and Peng Cui. Nico++: Towards better benchmarking for domain generalization. In *Proceedings of the IEEE/CVF Conference on Computer Vision and Pattern Recognition*, pages 16036–16047, 2023.
- [97] Xingxuan Zhang, Jiansheng Li, Wenjing Chu, Junjia Hai, Renzhe Xu, Yuqing Yang, Shikai Guan, Jiazheng Xu, and Peng Cui. On the out-of-distribution generalization of multimodal large language models. *arXiv preprint arXiv:2402.06599*, 2024.
- [98] Bingchen Zhao, Shaozuo Yu, Wufei Ma, Mingxin Yu, Shenxiao Mei, Angtian Wang, Ju He, Alan Yuille, and

- Adam Kortylewski. Ood-cv: A benchmark for robustness to out-of-distribution shifts of individual nuisances in natural images. In *Computer Vision – ECCV 2022*, pages 163–180, Cham, 2022. Springer Nature Switzerland.
- [99] Haozhe Zhao, Zefan Cai, Shuzheng Si, Xiaojian Ma, Kaikai An, Liang Chen, Zixuan Liu, Sheng Wang, Wenjuan Han, and Baobao Chang. Mmicl: Empowering vision-language model with multi-modal in-context learning. *arXiv preprint arXiv:2309.07915*, 2023.
- [100] Yunqing Zhao, Tianyu Pang, Chao Du, Xiao Yang, Chongxuan Li, Ngai-Man Man Cheung, and Min Lin. On evaluating adversarial robustness of large vision-language models. *Advances in Neural Information Processing Systems*, 36, 2024.
- [101] Kaiyang Zhou, Ziwei Liu, Yu Qiao, Tao Xiang, and Chen Change Loy. Domain generalization: A survey. *IEEE Transactions on Pattern Analysis and Machine Intelligence*, 45(4):4396–4415, 2022.
- [102] Xingyi Zhou, Dequan Wang, and Philipp Krähenbühl. Objects as points. *arXiv preprint arXiv:1904.07850*, 2019.
- [103] Chenchen Zhu, Yihui He, and Marios Savvides. Feature selective anchor-free module for single-shot object detection. In *Proceedings of the IEEE/CVF conference on computer vision and pattern recognition*, pages 840–849, 2019.
- [104] Xinge Zhu, Jiangmiao Pang, Ceyuan Yang, Jianping Shi, and Dahua Lin. Adapting object detectors via selective cross-domain alignment. In *Proceedings of the IEEE/CVF Conference on Computer Vision and Pattern Recognition (CVPR)*, 2019.
- [105] Xizhou Zhu, Weijie Su, Lewei Lu, Bin Li, Xiaogang Wang, and Jifeng Dai. Deformable detr: Deformable transformers for end-to-end object detection. *arXiv preprint arXiv:2010.04159*, 2020.